REVIEWS OF
MODERN PHYSICS

VOLUME 8 JULY, 1936 NUMBER 3

Electron Diffraction by Gas Molecules*

L. O. BROCKWAY, *Gates Chemical Laboratory, California Institute of Technology*

TABLE OF CONTENTS

I. INTRODUCTION

THE study of collisions of electrons with matter was begun by Lenard[1] more than forty years ago but the development of such experiments as a means of studying the structure of matter was delayed until the occurrence of three events some thirty years later. The first of these was observations made by Davisson and Kunsman[2] on electrons scattered by a polycrystalline nickel surface which with the subsequent experiments of Davisson and Germer[3] on electron scattering by single crystals of nickel were later interpreted as showing interference effects in electron scattering. The second event was the proposal of the theory by de Broglie[4] that associated with the propagation of material particles is a characteristic wave whose wave-length is determined by the mass and velocity of the particles. The third major event of this period was the introduction of the modern quantum mechanics by Heisenberg and Schrödinger which ultimately led to the development of a more or less complete theory of the relation between intensity and angle of scattering of electron beams falling on atoms or molecules.

Not long after the work of Davisson and de Broglie the application of electron diffraction to the study of crystal structure was tested by

* Contribution No. 549 from Gates Chemical Laboratory, California Institute of Technology.

Thomson[5] and Kikuchi.[6] Thomson bombarded foils of gold, silver, aluminum, and other substances with high velocity electrons (30 to 50 kilovolts) and found that the "wave-length" of his electron beams obeyed the de Broglie relation and that the diameters of the rings on his powder photographs could be accounted for on the basis of the structures for the various substances previously determined by x-rays. Kikuchi performed similar experiments on thin slips of mica.

In 1929 and 1930 Mott[7] derived a theoretical expression for the interaction of high velocity electrons with atoms in a form which could be easily used; and Thomson[8] and Mark and Wierl[9] studied the "atom form factor" for electrons by observing the relative intensities of the rings in the electron diffraction patterns produced by thin metal foils. In 1931 Wierl[10] published the results of an investigation on the molecular structures of twenty compounds in which high velocity electrons were diffracted by the respective compounds in the gaseous state. Since that time electron diffraction by gas molecules has come to be recognized as a powerful tool for the study of molecular structure.

The three hundred and fifty papers which have appeared in the field of electron diffraction since 1930 fall into four groups. The first, of about fifty papers, includes those in which the structures of single molecules are studied. High velocity electrons are used and the substances are studied as gases so that the result of the experiments is a knowledge of the atomic arrangement and the interatomic distances within single molecules. The electronic structure of atoms plays a negligible role here. This special branch of electron diffraction forms the subject of the present paper.

The second group of about sixty-five papers deals chiefly with monatomic gases interacting with low velocity electrons, generally less than a thousand volts. This work includes the well-known Ramsauer effect. Here the electronic distribution in atoms is important and the interest lies in the atomic cross sections defined by an angular scattering function and the excitation and ionization of atoms by the colliding electrons. Some polyatomic gases[11] also have been bombarded with low velocity electrons. Since the atomic scattering factors are not very well known for slow electrons the spatial arrangement of the atom centers (the nuclei) cannot be deduced from the diffraction of low velocity electrons by molecules. The nuclei are more effectively shielded by the extra-nuclear electrons in the diffraction of slow electrons, and the electronic structure of the molecule more nearly determines both the elastic and inelastic scattering than it does in the scattering of high velocity electrons. Only for the case of H_2 [12] has a complete theoretical treatment of the scattering been given. This second type of electron diffraction by gas molecules will not be discussed in this paper since it falls into an entirely different field of interest from the first type.

The third group of electron diffraction experiments comprising about one hundred and fifty publications to date involves the diffraction of high velocity electrons by solids, including crystalline powders, single crystals of metals and minerals, crystalline and amorphous organic substances and surface layers. Certain new types of diffraction phenomena have been observed.[13] Here again the chief interest lies in atomic arrangements and new results have been obtained in the important field of surface structure. The lower penetrating power of electrons as compared with x-rays makes the former particularly adapted to the study of surface characteristics. Studies have been made of the "inner potentials" of crystals which cause the electrons to have different velocities inside and outside of the crystal.

The fourth group consists of miscellaneous subjects including certain theoretical aspects not treated in the foregoing groups, theoretical and experimental work on electron polarization, determination of physical constants, tests of the de Broglie relation at very high velocities, etc.

Before the detailed discussion of electron diffraction by gas molecules is introduced, mention should be made of the interests largely motivating workers in the field and determining the scope of this paper. The need for solving many problems in structural chemistry really led to the development of this field since it afforded direct answers to some questions of long standing. Examples of these are the configurations of geometric isomers, the tetrahedral arrangement of bonds in aliphatic carbon derivatives, the planar character of the benzene ring, the angles between chemical bonds

on atoms of the various elements and the more recent considerations of the relation between the internuclear distance of chemically bonded atoms and other properties of the bond, such as electronic structure, force constant, dissociation energy, electric moment, etc. As a result the experimental method has been used primarily as a means of determining the structures of molecules. Those features have been tested thoroughly which are essential in affording a method for the determination of interatomic distances which will give reasonably accurate results and at the same time be simple enough to make practicable its application to a large number of compounds. The two requirements that the method yield accurate interatomic distances and be straightforward in application have not led to a complete quantitative comparison of the observed and theoretical intensities of scattering. Only in the case of benzene[14] has the comparison for relative intensities been carried out over a continuous range of scattering angle. In Section IV where procedures for interpreting the diffraction patterns are discussed it is shown that one which would give a complete test for the validity of the theoretical formulas for intensity of electron scattering would not be useful in determining interatomic distances.

The work done in the field has been determined by the interests outlined above, and the following treatment is addressed to future workers with these interests and to those who wish a general understanding of the field or who want to make independent estimates of the validity of the results. With the exception of the scattering of low velocity electrons, however, no aspect of electron diffraction by gas molecules has been neglected.

II. Theory

Elastic scattering by an atom

A theoretical expression is desired which will show the interference effects between the electrons scattered by the various atoms in a molecule. For this reason we consider first the elastically scattered electrons and subsequently the aggregate effect of all the different kinds of inelastic scattering. For the case of elastic scattering a single atom is treated and then a group of atoms having fixed relative positions, i.e., a molecule. The following solution of the problem of scattering by an atom is given in the form first used by Mott.[7]

The situation consists of a beam of electrons of uniform velocity traveling in a given direction in a field-free space. The electrons are scattered by an atom, which is represented by a small region within which there is a central force field, and the distribution of the scattered electrons is observed at great distances from the atom. If r is the distance of the point of observation from the atom, θ is the angle which the path of the scattered electron makes with the direction of the incident beam and N is the number of electrons in the incident beam crossing unit area per unit time, then the number of electrons falling on a small area dS per unit time is given by

$$NI(\theta)(dS/r^2) \equiv NI(\theta)d\omega.$$

$I(\theta)$ is the function to be calculated.

The problem is treated with the aid of the Schrödinger amplitude equation,

$$\nabla^2\psi(x, y, z) + (8\pi^2m/h^2)(W - V(x, y, z))\psi(x, y, z) = 0. \quad (1)$$

The symbol ∇^2 represents in Cartesian coordinates the operator $\partial^2/\partial x^2+\partial^2/\partial y^2+\partial^2/\partial z^2$. The solution ψ is a function of the coordinates x, y, and z with the origin taken at the center of the atom and $|\psi|^2$ will represent the distribution of electrons in both the incident and scattered beams. W is the kinetic energy of the electrons in the beam and is constant with the same value before and after the collision. W is determined by the potential used in accelerating the electrons for producing the beam. V is the potential energy of the interaction of the electron with the charged particles composing the atom and is assumed to be a function only of r, i.e., the atom is treated as spherically symmetrical.

The amplitude equation, whose solutions are not functions of the time, is used here because we are interested in $|\psi|^2$ for a steady state, i.e., W is the same throughout the scattering process. The factor $e^{(2\pi i/h)Wt}$ taken in conjunction with the solutions we shall obtain is known to lead to satisfactory solutions of the Schrödinger wave equation including the time but because we are interested only in the probability distribution of

scattered electrons we shall neglect the time factor.

For large r the desired solution of (1) must have the following form

$$\psi \sim e^{ikz} + (e^{ikr}/r) f(\theta). \tag{2}$$

The first term represents the incident plane wave traveling along the z-axis and is a solution of the equation for a free electron

$$\nabla^2\psi + k^2\psi = 0. \tag{3}$$

Eq. (3) is in the form of a classical wave equation and the constant k^2 which is a function of W may be related to a wave-length; that is,

$$k^2 = 8\pi^2 m W/h^2 = 4\pi^2/\lambda^2.$$

Expressing the kinetic energy in terms of velocity and mass, we obtain the de Broglie relation

$$\lambda = h/mv.$$

The second term in (2) represents the scattered wave and it follows that

$$I(\theta) = |f(\theta)|^2.$$

If Eq. (1) is rewritten in the form

$$\nabla^2\psi + k^2\psi = (8\pi^2 m/h^2) V\psi, \tag{4}$$

then the most general solution can be written in the form[15]

$$\psi = \psi_0 - \frac{1}{4\pi}\int \frac{\exp(ik|\mathbf{r}-\mathbf{r}'|)}{|\mathbf{r}-\mathbf{r}'|}\frac{8\pi^2 m}{h^2} V'\psi' d\tau' \tag{5}$$

if ψ_0 is the general solution of Eq. (3).

If the integral in (5) can be used to represent the scattered wave the quantities under the integral sign can be interpreted in the following way. The vector $\mathbf{r}$ extends to the volume element $d\tau'$, which contains scattering matter. V' and ψ' represent $V(x', y', z')$ and $\psi(x', y', z')$, respectively. The integrand can then be said to represent the amplitude and phase at the point $\mathbf{r}$ of the wavelet which was scattered in $d\tau'$ and which at unit distance had the amplitude $(2\pi m/h^2) V'\psi' d\tau'$. The integral is the summation of the wavelets produced by all of the scattering matter and will have contributions from all of the volume in which $V(x', y', z')$ is different from zero. The primed coordinates in (5) thus refer to the atom and the unprimed coordinates to the scattered wave. Fig. 1 shows the relation of these coordinates.

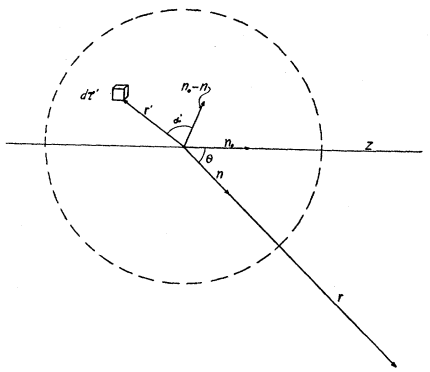

FIG. 1. Coordinates in atomic scattering.

The first term of (5) must represent the incident wave. This is compatible with the definition of ψ_0 (i.e., a solution of (3)) and we choose an infinite plane wave traveling along the z-axis, so that

$$\psi_0 = e^{ikz}.$$

The condition upon which (5) is an acceptable solution is that the integral have the proper asymptotic form as given by the second term of (2). Since the point of observation is always a great distance from the atom, $r \gg r'$ and we may write

$$|\mathbf{r}-\mathbf{r}'| \sim r - (\mathbf{r}/r)\cdot\mathbf{r}'.$$

The integral becomes

$$\frac{-2\pi m}{h^2}\frac{e^{ikr}}{r}\int \exp(-ik(\mathbf{r}/r)\cdot\mathbf{r}') V'\psi' d\tau', \tag{6}$$

Accordingly the asymptotic form of (5) for large r has the form of (2) with

$$f(\theta) = (2\pi m/h^2)\int \exp(-ik(\mathbf{r}/r)\cdot\mathbf{r}') V'\psi' d\tau'. \tag{7}$$

This integral is a function only of θ since the unprimed coordinates appear only in the form $\mathbf{r}/r$, a unit vector at the angle θ to the direction of the incident beam.

The evaluation of (7) now requires the use of the Born approximation. ψ' is composed of two parts, ψ_0' and an integral corresponding to the

one in (5). The approximation consists in neglecting the integral expression, that is,

$$\psi' \sim \psi_0' = e^{ikz'}. \tag{8}$$

This is equivalent to saying that inside the atom the amplitude of the incident wave is much greater than that of the scattered wave, or that the wave scattered by one part of the atom will not be scattered again by another part of the atom. Furthermore, no phase shift occurs in the scattering process. The limitations imposed on the final result by this approximation are discussed below.

If we set $z' = \mathbf{n}_0 \cdot \mathbf{r}'$ where $\mathbf{n}_0$ is a unit vector along the z-axis and let $\mathbf{n}$ represent the unit vector $\mathbf{r}/r$, then substitution of (8) in (7) gives

$$f(\theta) = \frac{2\pi m}{h^2} \int \exp\,(ik(\mathbf{n}_0 - \mathbf{n}) \cdot \mathbf{r}')\, V' d\tau'. \tag{9}$$

In order to perform the integration we first rewrite the exponent. Since θ is the angle between $\mathbf{n}_0$ and $\mathbf{n}$, the absolute value of $\mathbf{n}_0 - \mathbf{n}$ is equal to $2 \sin \theta/2$, and

$$k(\mathbf{n}_0 - \mathbf{n}) \cdot \mathbf{r}' = 2k\,(\sin \theta/2) r' \cos \alpha',$$

in which α' is the angle between $\mathbf{r}'$ and the vector $(\mathbf{n}_0 - \mathbf{n})$. Taking this vector as the polar axis and dropping the primes we integrate (9).

$$f(\theta) = \frac{2\pi m}{h^2} \int_0^{2\pi} d\beta \int_0^{\pi} \sin \alpha d\alpha \int_0^{\infty} e^{i2k\,(\sin \theta/2) r \cos \alpha} \times V(r) r^2 dr$$

$$= \frac{8\pi^2 m}{h^2} \int_0^{\infty} \frac{\sin sr}{sr} V(r) r^2 dr, \tag{10}$$

in which

$$s = 2k \sin \theta/2 = 4\pi (\sin \theta/2)/\lambda.$$

Since $V(r)$ is the potential due to the atomic field, it may be expressed in terms of the charge density in the atom;

$$V(r) = -\frac{Z\epsilon^2}{r} + \epsilon^2 \int \frac{|\phi(r')|^2}{|\mathbf{r} - \mathbf{r}'|} d\tau'. \tag{11}$$

The first term is due to a nucleus with charge $Z\epsilon$ and the second is due to the electron distribution in the atom; $\phi(r')$ is the solution of the Schrödinger equation for an atom with a spherical distribution of charge.

Expression (11) may be substituted in (10) and the final result is obtained by a two-stage integration by parts. An alternative procedure for obtaining the same result makes use of a formula due to Bethe[16] in the following form

$$\int \frac{\exp\,(ik(\mathbf{n}_0 - \mathbf{n}) \cdot \mathbf{r})}{|\mathbf{r} - \mathbf{r}'|} d\tau = \frac{4\pi \exp\,(i(\mathbf{n}_0 - \mathbf{n}) \cdot \mathbf{r}')}{k^2 |\mathbf{n}_0 - \mathbf{n}|^2}. \tag{12}$$

If expression (11) is substituted in (9) and simplified by (12), we obtain[17]

$$f(\theta) = \frac{8\pi^2 m\epsilon^2}{h^2} \frac{1}{s^2} \left[Z - 4\pi \int_0^{\infty} |\phi(r)|^2 \frac{\sin sr}{sr} r^2 dr \right]$$

$$= \frac{8\pi^2 m\epsilon^2}{h^2} \frac{Z - F(\theta)}{s^2}, \quad s = 4\pi \frac{\sin \theta/2}{\lambda}, \tag{13}$$

where $F(\theta) = 4\pi \int_0^{\infty} |\phi(r)|^2 ((\sin sr)/sr) r^2 dr.$

The complete solution of the problem is

$$\psi = e^{ikz} + (8\pi^2 m\epsilon^2/h^2)(e^{ikr}/r)((Z - F)/s^2). \tag{14}$$

F is identical with the atomic scattering factor of x-rays and numerical values have been tabulated for all atoms.[18] It is the fact that the properties of the function F have previously been studied which makes (13) an especially convenient form for the expression of the scattering of electrons by an atom.

$F(\theta)$ tends toward zero with increasing s so that for short wave-lengths (high velocity electrons) and large angles the scattering is done chiefly by the nucleus, or one may say that of the electrons penetrating the atoms those which pass closer to the nucleus will be scattered at larger angles.

At $\theta = 0$, $F(\theta)$ becomes equal to Z but $f(\theta)$ remains finite as has been verified with the aid of analytical expressions for $\phi(r)$ for hydrogen-like atoms with screening constants.[18b]

Validity of the Born approximation

A theoretical test for the conditions under which the Born approximation is valid requires the solution of the problem by an exact method and the comparison of the two results. For our

present purposes we refer to the complete treatment in Chapter II and the comparison with the result of the Born approximation in Chapter IV of Mott and Massey.[17] The test developed there is that

$$\frac{4\pi^3 m}{h^2}\int_0^\infty V(r)[J_{n+\frac{1}{2}}(kr)]^2 r dr \ll 1 \text{ for all } n. \quad (14a)$$

$V(r)$ is the potential field of the atom and $J_{n+\frac{1}{2}}(kr)$ is the Bessel function which occurs in the expansion of $(\sin sr)/sr$. The index n designates the successive terms in the infinite series contained in the exact formula for $f(\theta)$. Mott and Massey point out that the condition (14a) is very often too severe since in many cases it is violated for only the first few values of n, a fact which does not always introduce an appreciable discrepancy between the results of the exact formula and the Born approximation.

In terms of the energy of the bombarding electrons we should expect the approximate formula to hold better for higher energies, since V has been treated as a small perturbing potential. Numerical calculations[19] show that (14a) is sufficiently well satisfied by electron energies of a few hundred volts in the scattering by light atoms. For atomic numbers of about fifty or greater energies of the order of ten thousand volts are required. Since nearly all of the investigations of molecular structure by electron diffraction have been performed with the use of forty to fifty kilovolt electrons the Born approximation offers no difficulty in this field and hence the formula resulting from its application is greatly superior to the exact formula mentioned in the preceding paragraph whose application to the problems under discussion would be laborious in the extreme.

Elastic scattering by molecules

The diffraction by gas molecules is observed under experimental conditions such that the incident beam falls on a large number of molecules which have completely random orientations with respect to each other. The concentration of the gas molecules is small enough so that each molecule scatters independently of the others. The scattering is treated by calculating the effect for a single molecule in a fixed orientation and then averaging the result over all possible orientations. The movement of the molecule during the scattering process can be neglected.

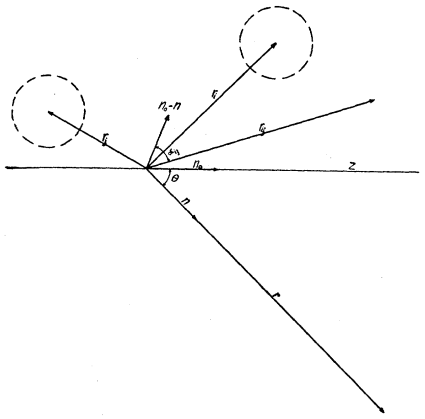

FIG. 2. Coordinates in molecular scattering.

The single molecule contains m atoms each of which scatters electrons according to Eq. (14). This requires the assumptions that the V function for each atom receives no contribution from the other atoms and that it remains spherically symmetrical. It is true that with the formation of chemical bonds neither of these assumptions holds but for the scattering of fast electrons the electronic structure of the molecule (or its atoms) plays a very minor role.

According to (14) the amplitude and phase of the scattered wave is given by $(e^{ikr}/r)f(\theta)$. If we refer the coordinates to an origin in the molecule which in general will not lie at the center of an atom and denote the coordinates of the ith atom by subscript i, then the wave scattered by the ith atom is

$$\psi_i = [\exp(ik|\mathbf{r}-\mathbf{r}_i|)/|\mathbf{r}-\mathbf{r}_i|]e^{ikz_i}f_i(\theta).$$

$\mathbf{r}$ is the vector to the point of observation and $\mathbf{r}_i$ to the center of the ith atom. Since the phase of the scattered wave depends on the phase of the incident wave the factor e^{ikz_i} is required. (Fig. 2.)

As before $r \gg r_i$ so that

$$|\mathbf{r}-\mathbf{r}_i| \sim r - \mathbf{n}\cdot\mathbf{r}_i,$$

where $\mathbf{n}$ is a unit vector along $\mathbf{r}$.

Then $\psi_i=(e^{ikr}/r)\exp(ik(z_i-\mathbf{n}\cdot\mathbf{r}_i))f_i(\theta)$

$=(e^{ikr}/r)\exp(ik(\mathbf{n}_0-\mathbf{n})\cdot\mathbf{r}_i)f_i(\theta).$

The sum of the scattered waves due to the atoms will represent the scattered wave due to the molecule,

$$\Psi=\sum_i\psi_i=\frac{e^{ikr}}{r}\sum_i\exp(ik(\mathbf{n}_0-\mathbf{n})\cdot\mathbf{r}_i)f_i(\theta). \qquad (15)$$

Because there are random phase relations between the waves scattered by different molecules the average over all possible orientations is to be taken on the square of the amplitude function for a single molecule. Accordingly, we first obtain the expression for $|\psi|^2$.

$$I=\Psi\Psi^*=\frac{1}{r^2}\Big[\sum_i\exp ik(\mathbf{n}_0-\mathbf{n})\cdot\mathbf{r}_i)f_i(\theta)\Big]^2$$

$$=\frac{1}{r^2}\sum_i\sum_j f_if_j\exp(ik(\mathbf{n}_0-\mathbf{n})\cdot\mathbf{r}_{ij}), \qquad (16)$$

where $\mathbf{r}_{ij}=\mathbf{r}_i-\mathbf{r}_j$, the separation of the ith and jth atoms in the molecule.

The orientation of the molecule may be designated by any one of the vectors $\mathbf{r}_{ij}$ and the averaging is carried out by integrating each member of the double summation over the angle variables in spherical polar coordinates referred to the vector $(\mathbf{n}_0-\mathbf{n})$ as the polar axis.

$$I(\theta)=\frac{1}{r^2}\sum_i\sum_j f_if_j\frac{1}{4\pi}\int_0^{2\pi}d\beta_{ij}\int_0^{\pi}d\alpha_{ij}e^{isr_{ij}\cos\alpha_{ij}}$$

$$=\frac{1}{r^2}\sum_i\sum_j f_if_j\frac{\sin sr_{ij}}{sr_{ij}}, \qquad (17)$$

where

$f_i=(8\pi^2me^2/h^2)((Z-F)_i/s^2)$,

$s=4\pi(\sin\theta/2)/\lambda$,

$r_{ij}=$distance between the ith and jth atoms.

This formula (with the exception of the factor f_i) was derived by Debye[20] and independently by Ehrenfest[21] in 1915 for the scattering of x-rays by molecules.

It is evident from (17) that $I(\theta)$ is a function of the structure of the molecule. The summations extend over all the atoms so that there is one term for each internuclear separation. The terms with $i=j$ reduce to f_i^2.

Inelastic scattering

The inelastic scattering of electrons by molecules may occur in several ways; the molecule may be lifted to any one of a number of excited electronic states (which may or may not lead to dissociation of the molecule), it may lose an electron and be ionized or in the case of very slow bombarding electrons the molecule may gain an electron, the molecule may also suffer a change in vibrational or rotational energy. The problem of interest here is the effect on the electron beam of scattering processes in which these energy changes may occur. Of special interest in the application of electron diffraction to the study of molecular structure is the question of coherence among the scattered waves or the appearance in the inelastic scattering of interference effects dependent on the structure of the molecule.

The answer to this question is found in the fact that the experimental observation is to be made on the aggregate effect of all inelastic processes. Interference effects do occur[22] when the molecule is excited to a definite state and the electrons are all scattered with the same wave-length change. The total effect, however, when the excitation of all possible states above the normal state is considered, produces incoherence in the scattered beam. The excitation of the molecule to vibrational and rotational states adjacent to the initial state without a change in electronic structure is possible when the energy of the bombarding electrons is smaller than that required to excite electronic changes. For fast electrons (i.e., with energy greater than the largest ionization potential of the heaviest atom in the molecule) the excitation of the scattering molecules to a small number of discrete levels is no longer possible. Accordingly under the conditions of the experiment, the inelastic scattering will also be incoherent and no diffraction effects related to the structure of the molecule will appear.

It is still desirable, however, to have an expression for the angular distribution of the inelastically scattered electrons since they furnish a background which must be included with the elastic scattering in the calculation of the total scattering. No treatment has been given as yet for the aggregate effect of the inelastic scattering by molecules but it seems probable that the result would not be much different from that of

treating the atoms separately and then summing over the atoms in the molecules. Such a treatment has been given by Morse[23] who shows that the incoherent scattering function for x-rays derived by Heisenberg[24] is applicable to the scattering of fast electrons if it is multiplied by the factor for the scattering due to a single electron, $(\sin\theta/2)^{-4}$.

The generalized expression for the intensity of the scattered beam which takes into account the wave-length change is

$$I(\theta)=\sum_l A^2\frac{k_l}{k_0}\left[\int \Phi_l^*(\mathbf{r})\Phi_0(\mathbf{r})\,V(\mathbf{r},\mathbf{r}')\exp\left(i(k_l\mathbf{n}-k_0\mathbf{n}_0)\cdot\mathbf{r}'\right)d\mathbf{r}d\mathbf{r}'\right]^2. \quad (18)$$

The coordinates $\mathbf{r}$ and $\mathbf{r}'$ are those of the atomic electrons and the bombarding electron, respectively. k_0 and k_l are the wave numbers, $2\pi/\lambda_0$ and $2\pi/\lambda_l$, before and after the collision; $\Phi_l^*(\mathbf{r})$ is the wave function representing the state of the atom after the collision and $\Phi_0(\mathbf{r})$ is the wave function before. V is the potential of the bombarding electron in the field of the atom. $\mathbf{n}$ and $\mathbf{n}_0$ as before, are unit vectors in the direction of the scattered and incident beams. The subscripts l designate the particular state excited and the summation is carried out over all of the possible excited states. The subscripts 0 refer to the initial state which we may assume to be the ground state of the molecule. This expression includes the elastic scattering since it reduces to the formula obtained above when $l=0$.

Eq. (18) is readily derived from the Schrödinger equation for the complete system, i.e., the wave equation which contains explicitly the coordinates of both the incident and atomic electrons while the energy term is the sum of the energy of the atom in its ground state and the kinetic energy of the incident electron. The solutions are assumed to be separable into functions of the incident electron and other functions for the atom. By expressing the general solution in the "integral" form and using the Born approximation (18) is obtained.

Morse has evaluated (18) for the case of fast electrons where k_l may be set equal to k_0. The result has the form

$$I(\theta)=\left(\frac{8\pi^2me^2}{h^2}\right)^2\left\{\frac{(Z-F)^2}{s^4}+\frac{S(v)}{s^4}\right\}. \quad (19)$$

The first term is just the expression obtained above for the intensity of the elastically scattered wave (cf. Eq. (14)) and the second term contains $S(v)$, the incoherent scattering function for x-rays due to Heisenberg.[24] Bewilogua[25] has tabulated S/Z as a function of $v=sb$ where $b=0.176/Z^{\frac{1}{3}}$. S goes to zero with θ and rises to a value Z for large angles. S/s^4, however, goes to a large finite value when θ becomes zero and drops rapidly with increasing angle. The behavior of the two terms in (19) is accordingly very similar.

The complete expression for the diffraction of fast electrons by gas molecules is

$$I(\theta)=I_0\left(\frac{8\pi^2me^2}{h^2}\right)^2\left\{\sum_i\sum_j f_if_j\frac{\sin sr_{ij}}{sr_{ij}}+\sum_i\frac{S_i}{s^4}\right\}. \quad (20)$$

$I(\theta)d\omega$ = no. of electrons scattered into the solid angle $d\omega$ per unit time.
I_0 = no. of electrons crossing unit area per unit time in the incident beam.
$f_i=(Z-F)_i/s^2$, atomic scattering factor for electrons.
Z = atomic number.
$F=4\pi\int_0^\infty|\phi(r)|^2((\sin sr)/sr)r^2dr$, atomic scattering factor for x-rays.[18]
$s=4\pi(\sin\theta/2)/\lambda$.
r_{ij} = distance between ith and jth atoms in the molecule.
S = tabulated inelastic scattering function.[25]

The application of this formula to the study of molecular structure is discussed in Section IV.

Temperature effect

The effect of the thermal vibrations of the atoms has been investigated by James[26] for the case of x-ray diffraction by gas molecules. The results of his theoretical treatment are applicable to electron diffraction. James shows that the contributions to both the coherent and incoherent intensity due to the thermal vibration of the atoms can be expressed by a temperature factor applied to the coherent terms in formula (20). This factor is e^{-A} where

$$A=8\pi^2\overline{\delta r_{ij}^2}\left(\frac{\sin\theta/2}{\lambda}\right)^2.$$

The mean square of the change in the distance r_{ij} represented by $\overline{\delta r_{ij}^2}$ is a function of the temperature. When $i=j$, δr_{ij} is zero and the temperature

factor becomes unity. For distinct values of i and j, e^{-A} is less than unity and becomes smaller with increasing angle. The intensity formula with the temperature factor is

$$I=K\left\{\sum_i f_i^2+\sum_i\sum_j{}'f_if_j\frac{\sin sr_{ij}}{sr_{ij}}e^{-A}+\sum_i\frac{S_i}{s^4}\right\}.$$

The temperature factor affects the relatively small part of the total intensity represented by the primed double summation, in which the terms with $i=j$ do not occur.

James evaluated $\overline{\delta r_{ij}^2}$ by a treatment of the normal coordinates in diatomic molecules and in tetrahedral molecules of the XY_4 type. For CCl_4 and $SiCl_4$ he used the spectroscopically observed frequencies to obtain numerical values of $\overline{\delta r_{ij}^2}$ at different temperatures. The predicted effect on the intensity is small and James was unable to detect a temperature effect in x-ray photographs of $SiCl_4$ vapor taken at 100°C and at 300°C. Similar experiments on CCl_4 by van der Grinten[27] led to the same negative result.

It is evident that the temperature effect will be small in electron diffraction by gas molecules. In a recent note Degard, Pierard, and van der Grinten[28] state that in the electron diffraction pattern of CCl_4 the temperature factor correction is necessary in order to get agreement with the observed intensity in the outer part of the pattern. In any event the use of electron diffraction for interatomic distance measurements is not affected by the temperature factor.

One other point has yet to be mentioned. Formula (20) requires the use of high velocity electrons but still does not include the relativistic corrections. Electrons accelerated by thirty to sixty kilovolts are well within the upper and lower limits of (20). When the wave-length is calculated by means of the de Broglie relation the relativistic expression for the mass of the electron should be used.

III. Experimental Procedure

The observation of electron diffraction effects produced by gas molecules is relatively simple in principle. A beam of electrons is made to pass through a sample of the gas and allowed to fall on a recording device. In practice a number of precautions must be observed if clearly defined patterns are to be obtained. The electrons in the beam must have a very small range of velocities (i.e., wave-lengths) and the beam should be well collimated. The volume of the intersection of the beam with the gas sample must be small and this requires that the experiment be performed in a high vacuum to reduce the scattering of the electrons by molecules throughout the apparatus. The recording device is almost inevitably a photographic emulsion, since the complete pattern must be registered in a fraction of a second. The emulsion must be protected from x-rays and other radiation.

The general form of the apparatus introduced by Wierl[10] is still used. It consists of two parts: the electron tube and the diffraction chamber including the plate-holder. The electron tube generates the electron beam and is connected to the diffraction chamber only through a fine hole in the anode which collimates the beam. A jet of the gas whose structure is being investigated flows across the path of the beam and may be condensed in part on a cold surface and in part removed by the high vacuum pumps connected to the diffraction chamber. The plate-holder is arranged so that a fluorescent screen or a number of photographic plates may be brought successively in front of the beam.

The experimental technique will be illustrated by a description of an apparatus used in this laboratory with a brief explanation where a choice has been made between alternative forms of certain parts.

Both cold and hot cathode tubes have been used as electron sources. In the cold cathode tube the cathode consists of a plate which may have a flat or a slightly concave surface. The focusing of the electrons on the anode plate may be partially controlled by the curvature of the face of the cathode. In the chamber containing these two electrodes a residual gas pressure of about 10^{-2} mm is maintained. When the high potential is applied the gaseous discharge produces ions and electrons, the latter being accelerated to the anode.

The advantages usually claimed for this type of tube are that the tube may be very simple in construction, the extra electrical circuit of the hot cathode tube is avoided and there is an automatic focusing effect of the electron beam due to the

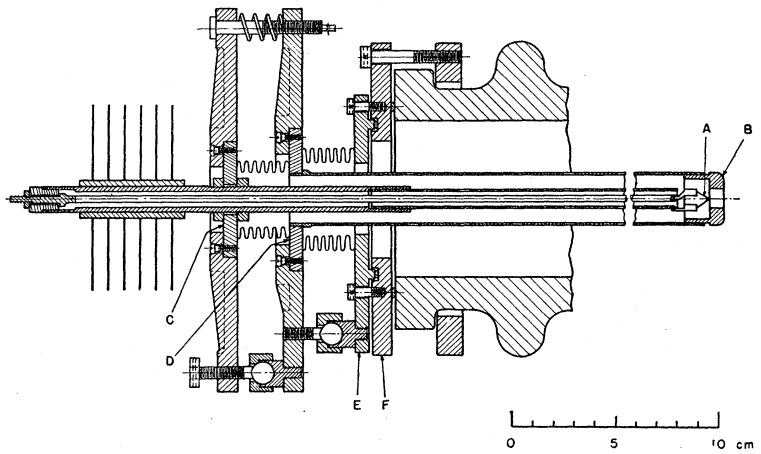

FIG. 3. Cathode assembly.

space charge in the tube. Tubes of this type have been used by most of the investigators in the field.

In the experience of the author the hot cathode tube offers a better control of the focusing of the beam, quite independent control of the space current and voltage, a steady discharge without the manipulation of gas leaks, much less power to be dissipated at the anode (about 1 percent of that in the gas tube) and even allows the use of unrectified a.c. potentials for accelerating the electrons. The tube described in the following embodies several distinctive features.

In Fig. 3 the cathode proper is the hair-pin shaped filament of 0.007″ tungsten wire at *A*. The ends are held in two clamping blocks mounted respectively on a one-eighth inch Monel rod and a $\frac{3}{8}$″ Monel tube. The rod is insulated from the tube by a glass sleeve at the filament end and mica sleeves and washers at the outer end, where the joint is made vacuum tight with Glyptal lacquer. The tube and the rod conduct the filament heating current. The tube is supported by an insulated joint at the plate *C*. The plate *D* supports a 1″ stainless steel tube which carries a cup *B* at the inner end enclosing the filament. The cup whose opening is $\frac{3}{8}$″ in diameter and $\frac{1}{4}$″ deep serves the purpose of focusing the electrons on the anode, which stands about an inch away. Because of the insulated joint in *C* a bias potential may be applied to the cup which is made about 200 volts negative with respect to the filament. The bias potential and the depth of the filament in the cup are adjusted so that the focal spot on the anode is not more than one millimeter in diameter.

The position of the filament in the cup is very critical in its effect on the beam. To provide an adjustment the plate *C* is connected to *D* by a flexible metal bellows and is supported by a ball and socket joint at one point and by screws working against stiff springs at two other points. With the aid of long insulated handles these screws may be operated while the high potential is applied to the cathode and the effect of the adjustment is observed on a fluorescent screen in the camera chamber. In the same fashion *D* is supported from *E* and this second adjustment moves the whole cathode with respect to the anode so that the focal spot may be brought onto the hole in the anode. *E* is supported by four short screws to the plate *F*, the joint being held tight by a gasket of special rubber. The cathode assembly is readily dismounted at this joint so that filament replacements can be made in a few minutes.

The condition that the electrons in the beam must all have very nearly the same velocity may

be met in several different ways. At the present time the most convenient source of high potential is a transformer, especially since used medical x-ray outfits can be purchased at a very reasonable price. The tube described above is capable of operating directly on the secondary output of such a transformer (Fig. 4). The secondary voltage is roughly sinusoidal but no current is carried during half of each cycle because of the self-rectifying feature of the hot cathode tube. During the other half-cycle the filament emits electrons which would be accelerated with all voltages from zero to the maximum value except for the effect of the negative bias on the focusing cup. This negative potential repels the electrons and prevents their leaving the cathode until the difference of potential between the filament and the anode exceeds a certain minimum value. With the arrangement shown a bias potential of 400 volts was sufficient to shut off the electron beam entirely against a peak potential of 50,000 volts at the anode. In operation the bias is lowered as much as possible without producing a serious inhomogeneity in the beam. This may be tested by observing on the fluorescent screen the effect of a magnetic field on the beam and also by the sharpness of the rings in photographs of gold foil. The temperature of the filament may be adjusted to give the desired current without requiring a readjustment of the bias potential. If the high potential is represented by a sine wave, current may be passed for 6 percent of each half-cycle with a fluctuation of less than $\frac{1}{2}$ percent in the voltage. The arrangement affords effective control of the beam and requires only high voltage equipment which will be found in almost any laboratory.

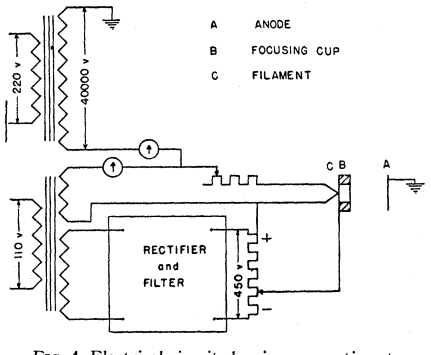

FIG. 4. Electrical circuit showing connections to focusing cup.

Another arrangement can be used in which the electron beam coming through the hole in the anode is passed through a magnetic field. A second slit or hole is placed at the point in the magnetic spectrum corresponding to the desired electron velocity. This method is less convenient than the foregoing one and the useful current is a small part of the total current.

The best high voltage supply is one which applies direct current to the electron tube. High voltage valves and condensers are available on the market and although the initial cost is objectionable the use of direct current has two important advantages. The first is that the fluctuation of the voltage can be held within very small limits; variations less than one-tenth of a percent are not difficult to maintain with a fairly simple filter system if the primary voltage is steady. The second advantage is that the voltage which is effective in determining the electron wave-length can be read with considerable accuracy at the instant of taking the photograph. This is accomplished with the use of a high resistance voltmeter.

About fifty megohms in high quality wire-wound resistors are placed in parallel with the electron tube and the potential drop is measured by the current in the resistors or by the drop across a small constant fraction of the total resistance. Such a voltmeter is especially useful in following fluctuations in the output of the high voltage supply. The ripple which has the same or twice the frequency of the alternating current used in the transformer may be reduced by using sufficient capacity in the filter circuit but variations due to unsteady frequency or voltage in the primary supply will be indicated by the voltmeter. These variations may be controlled manually or by a vacuum tube regulator which operates from the drop across a proportional part of the high resistance and applies compensating corrections to the primary voltage.

The absolute value of the voltage determines the wave-length used in the analysis of the photographs and therefore needs to be calibrated in terms of wave-length. The high resistance

meter just described can be used as a primary standard of voltage and the wave-length is then calculated by the relativistic form of de Broglie's relation combined with the assumption that the accelerating potential gives the electrons in the beam an equivalent kinetic energy. The formula then is the following,

$$\lambda=\left(\frac{150}{V}\right)^{\frac{1}{2}}\frac{h}{(\epsilon m_0)^{\frac{1}{2}}}\left\{1+\frac{\epsilon V}{600 m_0 c^2}\right\}^{-\frac{1}{2}}\text{cm},$$

$$=\left(\frac{150}{V}\right)^{\frac{1}{2}}\{1+9.834\cdot 10^{-7}V\}^{-\frac{1}{2}}\cdot A,$$

in which V is the accelerating potential in volts.

A second procedure is to calibrate the voltage measuring device directly in terms of wave-length by taking electron diffraction photographs of gold.[5, 9] A film thin enough to transmit the electrons is placed in front of the beam and because of the microcrystalline structure of the gold a powder photograph is obtained which is identical in the positions of its rings with photographs obtained by x-rays. The Bragg relation for cubic crystals,

$$\lambda=(2a_0\sin\theta/2)/(h^2+k^2+l^2)^{\frac{1}{2}}$$

allows the calculation of a value of the wave-length for each ring. a_0 is the edge of the cubic unit cell and has the value[29] 4.070A. θ is the deflection angle (between the incident and scattered beams, designated in x-ray scattering by 2θ). h, k, l are the Miller indices of the reflecting planes and for the face-centered lattice of gold h, k, l appear in all combinations in which they are all even or all odd. Table I illustrates the assignment of h, k, l values and calculation of wave-length from a photograph of gold leaf for which the electrons were accelerated by 39,600 volts d.c. Where two rings were unresolved an average value is used for $(h^2+k^2+l^2)^{\frac{1}{2}}$ in which the two forms are weighted according to the number of planes in the form. The direct calibration of wave-length by gold photographs is made for several voltages and repeated at intervals of a few months to check on the voltmeter.

TABLE I. *Calculation of wave-length from a gold photograph.* $L=12.91$ cm: $a_0=4.070$A.

Av. Dia. (mm)	(hkl)	$(h^2+k^2+l^2)^{\frac{1}{2}}$	$\sin\theta/2$	λ
6.64	111	1.732	0.02185	0.0604
7.65	200	2.000	0.01476	0.0601
10.81	220	2.828	0.02090	0.0602
12.79	311, 222	3.354	0.02470	0.0600
15.32	400	4.000	0.02967	0.0604
16.87	331, 420	4.415	0.03263	0.0602
18.74	422	4.899	0.0363	0.0603
20.02	511, 333	5.196	0.0388	0.0608
21.85	440	5.657	0.0422	0.0608
22.81	531, 600, 442	5.95	0.0441	0.0603
24.31	620	6.325	0.0470	0.0605
25.62	533, 622	6.60	0.0494	0.0609
27.46	711, 551, 640	7.16	0.0530	0.0603
29.42	731, 553	7.60	0.0568	0.0608
31.65	733, 820, 644	8.22	0.0609	0.0603 ½ wt.
33.48	751, 555, 662	8.68	0.0643	0.0603 ½ wt.
			AVERAGE	0.0604

The production of well-defined diffraction patterns as mentioned above requires that the electrons meet the gas in a small volume. The strong interaction of electrons with matter prohibits the use of even thin windows for confining the sample of gas but on the other hand it allows such short exposures to be used that there is no great difficulty in maintaining a flowing gas jet for the duration of the exposure. The problem arises of preventing the spreading out of the gas throughout the diffraction chamber, i.e., of maintaining a high vacuum (10^{-4} mm or less) in a region into which a jet of gas is flowing. The chamber will of course be evacuated by a good set of diffusion pumps but some special arrangement in addition must be provided for condensing or removing the gas introduced. Another precaution to be observed when a hot cathode tube is used is that of protecting the electron tube from the gas flowing into the diffraction chamber.

Fig. 5 shows the arrangement generally used in this laboratory. The apparatus is built up in sections from three-inch brass tubing. The joints are made by flanges which are threaded and sweated onto the tubing. They are held together by an arrangement of six push and six pull screws so that the axes of the individual sections can be accurately aligned. The joints which are made vacuum tight by rubber gaskets are interchangeable and extra sections may be used. In addition to the three sections illustrated the apparatus includes a diffraction and camera unit made for wide angle photographs and two sections used for increasing the distance from the diffraction point to the film.

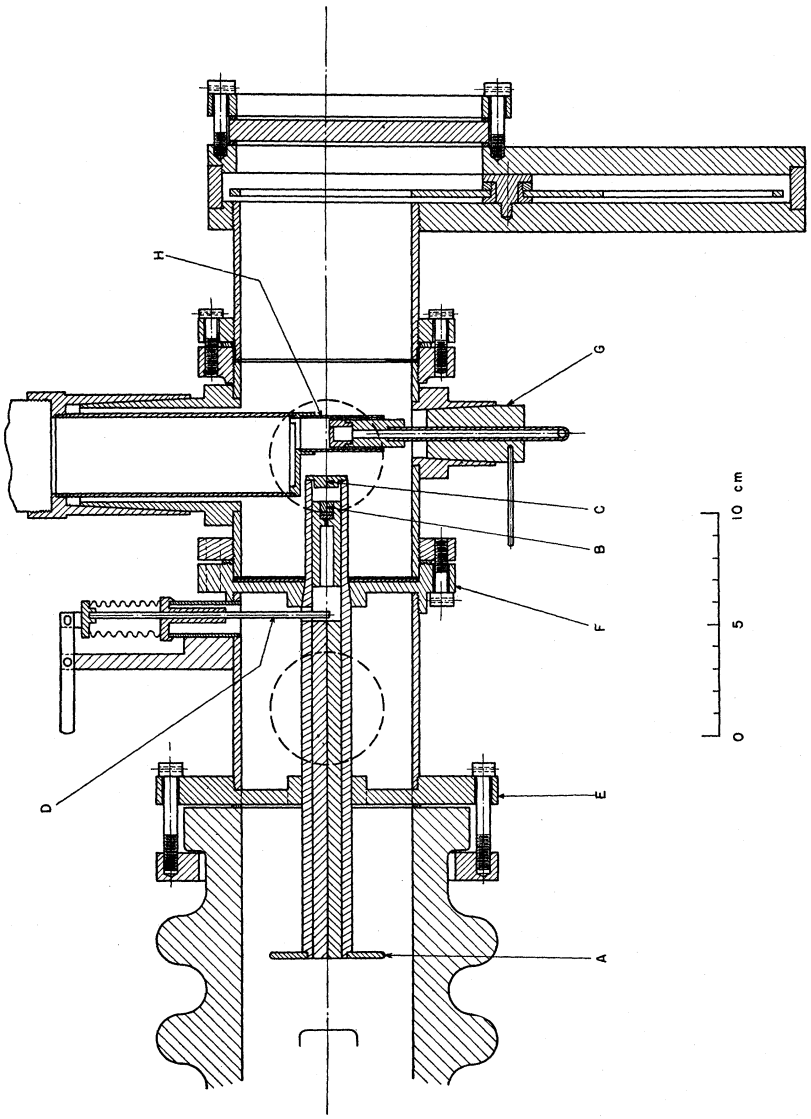

FIG. 5. Collimating system, diffraction chamber and camera.

Electrons from the filament strike the anode, *A*. In the center of the anode is a hole, 0.2 mm in diameter, which is the opening of a tube of that diameter and 15 cm long. This long hole together with the 0.4 mm hole at *B* and the 0.8 mm hole at *C* are the collimating system. The beam is defined by the long hole and the two short holes cut off the electrons which are diffracted at the end of the long hole. It has been found that for a given electron current striking in a given focal area on *A* the long tube transmits from ten to twenty times more electrons than two pin-holes of the same diameter in thin platinum placed at the positions of the ends of the long tube. *D* is a rod which is moved through a small metal bellows by a lever on the outside; this acts as a mechanical shutter for controlling the passage of the beam.

The first section of brass tube in Fig. 5 (enclosed between flanges *E* and *F*) is really a part of the electron tube. The flanges *E* and *F* are plates supporting the collimating system, which may be taken out as a unit through the cathode end when adjustments are required. The hole in *F* is tapered so that the collimator always returns to the same position and at the same time closes the connection between the diffraction chamber and the electron tube. The only passage for gas between the two chambers is through the holes at *B* and *C*. The section *EF* has a two-inch connection to the diffusion pumps which evacuate the electron tube and the position of this connection allows the small amount of gas coming through *B* and *C* to be pumped out before it affects the electron discharge. This is indicated by the steadiness of the space current at the time the gas is flowing in the diffraction chamber. The plate *E* which also supports the insulating procelain tube has four ports for the evacuation. The plate *F* is lined with lead as an x-ray shield for the camera.

The second section carries the gas nozzle. The nozzle illustrated is used for substances which have a high vapor pressure at about 40°C or any lower temperature. The tapered plug at *G* carries a tube with the upper end closed except for a 0.3 mm hole through which the gas emerges. The electron beam passes about 2 mm above the end of the nozzle. Below the plug the tube turns through 90° and connects through a tapered joint and glass stop-cock to the glass vessel containing the substance.

The gas emerging from the nozzle is directed into the opening of a high speed pump connection. The upper end of the nozzle is completely enclosed for about an inch by the pump connection tube *H* with a clearance of less than 0.5 mm. The electron beam passes through two holes in the tube *H* which are just large enough to clear the beam, allowance being made for the maximum scattering angle. The relatively large area of the two-inch pump connection compared to the openings out into the main body of the apparatus allows the greater part of the gas to be removed without an opportunity for it to affect the electron beam beyond the diffraction point. A separate pump is connected directly to the diffraction section (at the point indicated by the dotted circle in the figure) which serves for the evacuation of the diffraction chamber and camera.

The arrangement described has been found more effective in eliminating the diffuse scattering due to stray gas molecules than several others in which the gas was condensed on a surface cooled to the temperature of liquid air. In an attempt to improve the condensation a layer of charcoal was placed on the condensing surface but even this was not effective enough in condensing gases with very low melting points, such as CF_4. Another difficulty lies in the fact that the cold surface cannot be made to surround the gas jet as completely as the pump connection does without cooling the gas nozzle itself below the condensing point of many of the substances used and thereby plugging the nozzle.

The film-holder is a vertical disk with six three-inch holes over which five films and a fluorescent screen can be mounted. The disk is rotated from the outside by the action of a small magnet on pieces of iron mounted on the edge of the disk and the films are brought successively into position for exposure. The film-holder is mounted between two thick brass plates which are supported by a rim at the outer edge and a screw at the center on which the film-holder revolves. The back plate has an opening which serves both as a door through which the film-holder is loaded and as a window through which the fluorescent screen is observed. The

opening is covered by a glass plate and made vacuum tight by rubber gaskets.

The gas photographs are taken on x-ray film although any other emulsion of approximately the same properties can be used. The emulsion should have a low contrast and a long scale, i.e., it should be sensitive over a great range of intensities. Eastman Par Speed Portrait film works fairly well but although no quantitative tests have been made it seems to be a little slower than x-ray film. For gold photographs where the pattern is a series of sharp rings Process films are used in order to get a high contrast between the rings and the intervening background.

The diffusion pumps have a high pumping speed and short connections of large diameter to keep a low pressure in spite of the gas introduced. It is important that separate pumps be used on the electron tube and diffraction chamber. For the apparatus described above four metal diffusion pumps of the style described by Sloan, Thornton, and Jenkins[30] are used. They operate on Apiezon oil "B" and one with a body diameter of two and five-eighths inches and a jet clearance of a quarter of an inch is used as a first stage for backing the other three, all of which operate as second stage pumps with jet clearances of one-eighth of an inch. One of the second stage pumps is connected to the electron tube, the second to the diffraction chamber and the third to the tube surrounding the gas jet. The first two pumps have operated satisfactorily without liquid-air cooled traps although their use would undoubtedly decrease the ultimate pressure, according to the recent investigations of Hickman[31] on the designing of oil pumps for low ultimate pressures. An efficient trap cooled with liquid air has been inserted, however, in the line to the third pump and in it the vapors brought in through the gas nozzle are condensed. The trap is constructed so that the glass bowl containing the condensed vapors may be removed from the apparatus while the low temperature is maintained. In this way the pump oil is protected from contamination. Vapors which are not condensed by the liquid air will not affect the pump oil. The diffusion pumps are backed by a Cenco Megavac mechanical pump.

Exposures are made in the following manner. If the substance whose structure is to be studied can be readily condensed, it is placed in a small glass bulb which is connected to the nozzle through a stop-cock and a tapered ground joint. The camera is loaded and the pumps started. About half an hour after the diffusion pumps are hot the pressure is low enough. The high potential is set at some predetermined value in the neighborhood of 40,000 volts by means of the secondary voltmeter. The space current in the electron tube is set from 0.05 to 0.20 milliampere. The central spot is observed on the fluorescent screen and the bias potential and the filament position are adjusted until the spot shows its maximum intensity. These adjustments are very stable in the sense that only slight changes are required during several series of photographs. The shutter D is dropped and a film moved into position.

By means of a temperature bath the sample is brought to a temperature at which it has from 100 to 200 mm vapor pressure. The exposure is made by turning the stop-cock at the same time the shutter is opened for an instant. The stop-cock is turned through 180° in very nearly a second. The passage through the cock is open for about a fifth of a second and the shutter is opened and closed during that time. In a number of cases three or four such exposures are made on the same film at intervals of ten seconds or more. The resulting film shows on visual examination

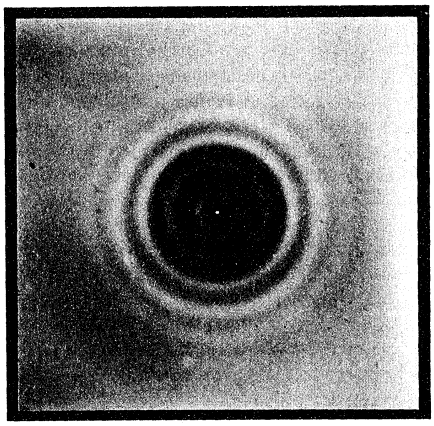

FIG. 6. Electron diffraction photograph of As_4 vapor. This photograph was taken by Dr. L. R. Maxwell of the U. S. Department of Agriculture.

a set of maxima and minima which are rather diffuse by comparison with the photographs of crystalline powders. Fig. 6 is a reproduction of a photograph of As_4 vapor.

If the substance has a very low boiling point the sample may consist of the vapor at about 200 mm pressure in a glass flask attached as before to the apparatus. If the sample has a very low vapor pressure below about 50°C a different nozzle arrangement is required since the gas will condense in the room temperature nozzle illustrated in Fig. 5 if the sample is heated above that temperature.

A well-designed apparatus using a gas discharge as electron source has been described by de Laszlo[32] which is being used in several European laboratories. He uses a very compact form of high temperature nozzle which is said to reach temperatures up to 1000°C. A small cylindrical oven with a removable head is mounted just under the electron beam and the vapor streaming out through a small hole in the oven-head intersects the beam. A number of other investigators have used high temperature nozzles of this general form. Nozzles of this form have one drawback in that they allow a stream of the vapor to flow continuously and hence introduce large volumes of gas into the apparatus which are not useful in producing photographic exposures. A desirable improvement is being developed in this laboratory whereby a valve located in the oven-head controls the flow of gas and is opened only during the exposure. This arrangement has been used successfully at 175°C and is being tested at higher temperatures.

A modification of de Laszlo's apparatus was made by Cosslett[33] in which a more effective condensation of the gas is arranged. He causes the gas to flow through a narrow tube and lets the electron beam pass through two holes in the tube, thus restricting the volume of intersection of the gas and electron beam. The gas is directed against a liquid-air cooled surface placed close to the end of the tube. If the gas conducting tube were connected to a pump the gas would have a still smaller chance of escaping into the diffraction chamber and camera.

Seemann of the Seemann Laboratory in Freiburg described an electron diffraction apparatus for solids[34] which was later adapted for use with gases according to Wierl's design. More recently Seemann has replaced the gas discharge tube with a cathode consisting of a hot filament and focusing cup. The apparatus and mounting are very compact and can be readily changed for use as a Lenard tube or as an x-ray tube. Its use in electron diffraction by gases is described by Grethier.[35]

IV. Interpretation of Photographs

Quantitative intensity measurements

The most generally used procedures for interpreting the photographs have been developed to yield accurate inter-nuclear distances and, since qualitative intensity measurements have sufficed for this purpose, no complete quantitative comparison of the observed and theoretical relations between intensity and angle of scattering has been made. Accurate intensity measurements would require the use of electrical methods of detecting the electrons but there are two difficulties with the use of electrical detectors. Observation of the diffraction pattern over a range of scattering angle would necessitate a series of individual measurements and as mentioned above to maintain a constant amount of scattering matter over a period of time in a volume small enough to give sharp diffraction patterns is difficult with gases. Moreover an electrical detector used in a vacuum apparatus of practical size would be close enough to the diffraction point so that it would collect all of the electrons within a little range of scattering angle and not distinguish their differences in direction. A photographic film on the other hand registers the complete pattern at once and it will detect intensity variations in directions separated by extremely small angles. Since the angular positions of characteristic features of the diffraction pattern are used in determining the size of the molecule an accurate reproduction of the geometry of the pattern is more important than are quantitative measurements of the intensity. For these reasons photographic films are especially suited to the purpose at hand.

Approximate quantitative intensities of electron beams can be measured by photographic emulsions and some work has been done on the behavior of various emulsions toward electrons.[36]

The reciprocity law which states that the photographic density is a function of the product of intensity and exposure time (i.e., total electrical charge per square centimeter in the case of electrons) holds for fast electrons if the exposure time is not varied more than about one hundred fold. If the photographic density (defined as the common logarithm of the reciprocal of the transmission) is plotted against the logarithm of the charge per square centimeter a characteristic curve is obtained similar to the curves found for visible light. A non-linear part with increasing slope in the region of small exposure is followed by a steeper, approximately linear region covering a range of from ten to one hundred-fold increase in charge beyond which the effect of saturation appears. The contrast (or the slope of the linear portion) increases and the inertia (or the intercept of the extended linear portion) decreases with increasing voltage so that maximum blackening is presumably reached at a lower charge density with higher voltages. This effect passes through a maximum, however, in the general neighborhood of one hundred kilovolts and for very high voltages the increase of blackening per unit charge falls off with increasing voltage. The characteristic curve for a photographic plate to be used in a particular experiment depends essentially on the velocity of the electrons and the kind and thickness of the emulsion with a possible effect of the nature of the backing in the case of very fast electrons.

The experiments quoted show that for the kinds of emulsions investigated at the electron velocities used in diffraction by gas molecules a range of from fifty to a hundred fold in exposure covers the characteristic curve from a blackening of 0.2 below which microphotometer measurements of the density are inaccurate up to a blackening of 1.5 to 2.0 beyond which the emulsions have not been studied. In the following paragraphs it is shown that the intensity of scattered electrons varies more than a thousand fold in the angular range which is of interest in certain compounds. Quantitative intensity measurements over this range could be tried on a series of photographs of different exposure times although no one has succeeded in raising the blackening in the outer part of the diffraction pattern high enough to be measured with a microphotometer without raising the background so much that the pattern is obscured. For example, the pattern due to CCl_4 has not been measured with a microphotometer record beyond the seventh order although orders as high as the twelfth have been observed visually.

Theoretical intensity curves for CCl_4

The intensity function which is to be compared with the photographs is given by Eq. (20). As an illustration this formula is now applied to the CCl_4 molecule. The assumption of a definite molecular model is required for the calculation of the intensity. In view of the tetahedral bond directions ascribed to the carbon atom by the organic and the theoretical chemists and in view of the observed zero dipole moment we may undertake to test the model having a carbon atom at the center and chlorine atoms at the vertices of a regular tetrahedron. Eq. (20) then becomes

$$I=K\left\{f_C^2+f_{Cl}^2\left(4+12\frac{\sin 2.87s}{2.87s}\right)+f_C f_{Cl}8\frac{\sin 1.76s}{1.76s}+\frac{S_C}{s^4}+\frac{4S_{Cl}}{s^4}\right\}. \quad (21)$$

The Cl−Cl distance has been taken as 2.87A and the C−Cl as 1.76A. The ratio of the Cl−Cl to C−Cl distances is fixed by the geometry of the model at 1.633 but the absolute values assumed in this formula are arbitrary. Definite values are chosen in order that I may be calculated as a function of s; and if the geometry of the model is correct the absolute size will be determined by the shift in the scale of abscissae for this function which is required to make it match the observed intensity curve. If the geometry of the model is incorrect there will be no possible shift in scale which will match the theoretical and observed curves. If the curve for the correct model leads to absolute distances which are appreciably different from the assumed values the new values may be inserted in the formula and a second curve calculated. By this procedure it is possible to approach the true values for the distances by a set of successive approximations.

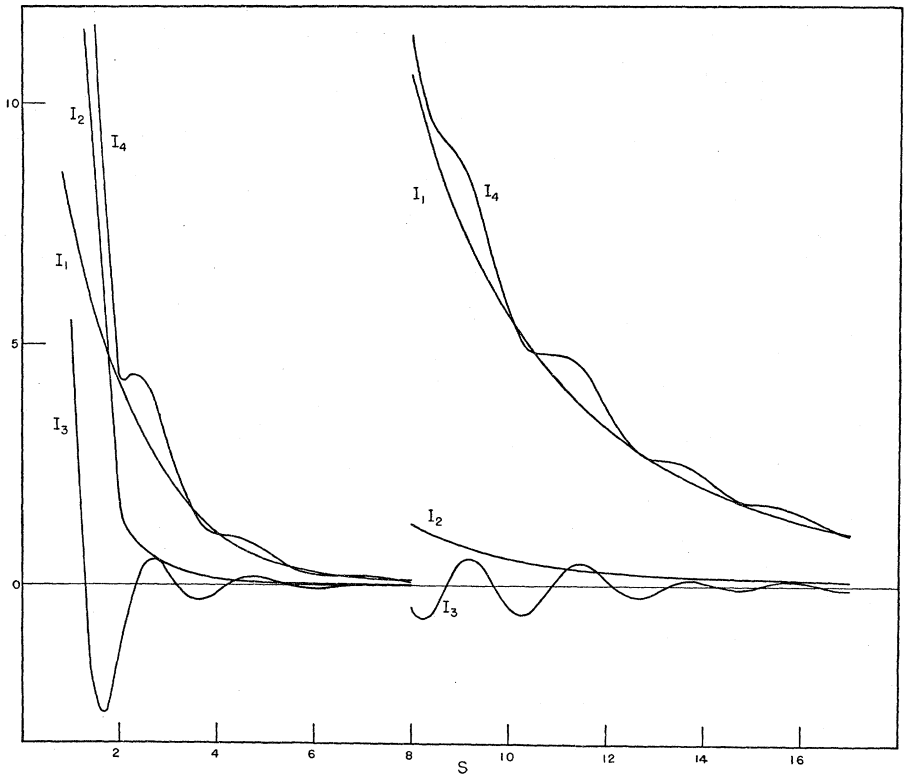

FIG. 7. Theoretical electron diffraction curves for CCl_4. The ordinates are multiplied by 100 beyond $s=8$.

In order to show the relative importance of the various terms in (21) the coherent atomic scattering, the incoherent atomic scattering, and the molecular scattering are plotted separately together with their sum in Fig. 7. The separation is as follows:

$I_1=f^2_C+4f_{Cl}$—coherent atomic scattering,

$I_2=\frac{S_C}{s^4}+4\frac{S_{Cl}}{s^4}$—incoherent atomic scattering,

$I_3=f^2_{Cl}12\frac{\sin 2.87s}{2.87s}+f_Cf_{Cl}8\frac{\sin 1.76s}{1.76s}$—molecular scattering,

$I_4=I_1+I_2+I_3$.

The scale of ordinates is fixed by setting the constant, K, in (21) equal to unity. The F values which occur in the f's were taken from Pauling and Sherman.[18b] The S values are from Bewilogua's table.[25] At $s=8$ the scale of all four curves is multiplied by a factor of a hundred. The curves are carried out to $s=17$ which includes the first seven "maxima" in the pattern for CCl_4.

It will be observed that although both of the atomic curves fall very rapidly with increasing angle the fall in the incoherent curve is much more pronounced than in the coherent. At very small angles the incoherent intensity is the greater part of the total intensity but for this compound it falls below the atomic coherent curve at $s=1.8$ and beyond the point $s=4$ the incoherent intensity is roughly ten percent of the coherent intensity. The incoherent scattering will be important near the central image but in

the outer part of the diffraction pattern it will play a very minor role.

Of especial interest is the curve I_3, the molecular scattering, since this is the only component of the total scattering which depends on the structure of the molecule. It consists of a sum of strongly damped sinusoidal curves but beyond the first maximum the heights of its maxima above the preceding minima are less than the decreases in the atomic background curve over the corresponding regions so that the total intensity does not show real maxima but only oscillations about the atomic background. The general form of this curve is confirmed by microphotometer records of the photographs (Fig. 8).

As mentioned above the test of this curve by a comparison of theoretical and observed intensities over the complete angle range has never been made. This is partly due to the difficulties encountered in the quantitative measurement of the intensities; it may be noted that in going from the first maximum at $s \approx 2.3$ to the tenth maximum at $s \approx 25$ the total intensity changes from 4.3 to 0.0027, a ratio of 1600 to 1. A more important reason is that such a test would not be useful in the application of the experiment to the study of molecular structure. The molecular scattering is such a small part of the total intensity that the total intensity is relatively insensitive to changes in the molecular scattering curve. That is to say that changes in the parameters determining the molecular model do not produce proportional changes in the calculated total intensity. Although good quantitative agreement might be found between a theoretical and an observed intensity curve that fact would not mean that the molecular structure was determined with corresponding accuracy. It would be necessary to find out how much the molecular model could be altered without producing definite disagreement between the corresponding calculated curves and the observed intensity.

For structure determination it is desirable to have a comparison between theory and experiment which is sensitive to changes in the scale of the molecular scattering curve. This will be true of the quantitative intensity comparison in the neighborhood of a well-marked shoulder on the curve where a real maximum actually or very nearly exists (such as the first hump in Fig. 7). The correct theoretical curve will be expected to reproduce the shape and position of this distinguishing feature on the observed curve, and the matching over the shoulder can be done with considerable accuracy with respect to variation in the size of the molecule. This procedure has been applied only in the case of benzene, by Pauling and Brockway.[14] The microphotometer records of the photographs show a pronounced second hump to which was fitted the corresponding hump in theoretical microphotometer records made by applying the microphotometer calibration in terms of intensity of incident electrons to the theoretical intensity curve. The final result supported a regular hexagonal model with a separation of adjacent carbon atoms equal to 1.39A. The photographs showed an extra background which was less steep than the incoherent scattering in the region measured and was due to multiple scattering and to scattering of electrons by gas molecules in the body of the apparatus. The disadvantage of this method is that it can be applied in only one small region of the curve for any given substance since in general

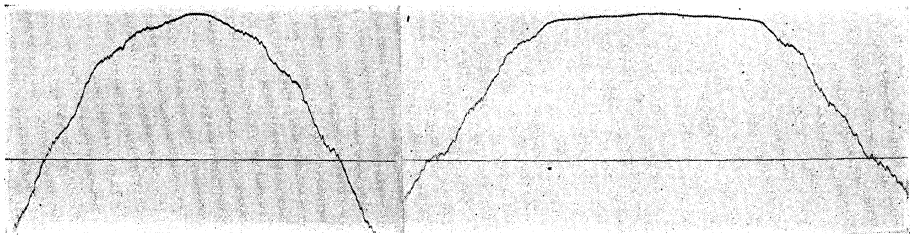

FIG. 8. Microphotometer records of CCl_4 photographs, (A) (left) showing the first three and (B) (right) showing the first five apparent maxima.

the humps on the total intensity curve are so broad and flat that even small uncertainties in the observed intensity have a marked effect on the shape of a hump and approximate fits can be obtained over too large a range of the molecular parameters.

The desired accuracy has been obtained by a number of variations of a second procedure. This consists of determining the s values of a number of points which fix characteristic features on a theoretical curve and correlating these with the corresponding points on the photograph. Although quantitative intensities are not used various qualitative intensity effects are correlated in the comparison of theory and experiment. Such methods involve less labor than the matching of quantitative intensities since the occurrence of background effects which do not fall off more rapidly than the atomic background has no effect on the measurements. All of these methods are tested for reliability by an empirical comparison of their results on certain compounds with the results obtained for the same compounds by other methods of investigation, especially band spectral analysis and x-ray diffraction. The variations differ in the manner of choosing the points to be correlated. Their relative merits are to be judged on the basis of accuracy of results and simplicity of application.

Visual method

The first method used by Wierl[10] is the so-called "visual" treatment. Under visual observation the photographs show sets of well-defined circular bands which apparently correspond to maxima and minima in the photographic blackening. In general such maxima and minima in the blackening do not exist but the eye is sensitive not to the total intensity of light transmitted by the negative under observation but rather to the ratio of the changes in the transmitted intensity to the total intensity. A detailed discussion of the behavior of the eye in relation to the appearance of electron diffraction photographs of gases has been given by Pauling and Brockway[37] from which it appears that the eye is sensitive to the fluctuations about a background to an extent approximately determined by the ratio of the fluctuation to the background and this is true for a large range of background intensities. These considerations not only explain the visual appearance of the photograph but indicate that the eye magnifies the effect of the contribution of the molecular scattering curve (I_3) to the total intensity, i.e., the visual appearance will be strongly characteristic of the structure of the molecule.

In the quantitative treatment the points correlated are the positions of the apparent maxima and minima on the photograph and the positions of the maxima and minima on a modified molecular scattering curve. In accordance with the treatment referred to in the preceding paragraph the theoretical curve should be (for the example of CCl_4)

$$\frac{I_{\text{mol}}}{I_{\text{atomic}}}=\frac{I_3}{I_1+I_2}=\frac{f_{Cl}^2(12\sin 2.87s)/2.87s+f_C f_{Cl}(8\sin 1.76s)/1.76s}{f_C^2+4f_{Cl}^2+(S_C+4S_{Cl})/s^4}$$
$$=\frac{(Z-F)_{Cl}^2(12\sin 2.87s)/2.87s+(Z-F)_C(Z-F)_{Cl}(8\sin 1.76s)/1.76s}{(Z-F)_C^2+4(Z-F)_{Cl}^2+S_C+4S_{Cl}}, \qquad (22)$$

in which the factor $1/s^4$ appearing in each term of the numerator and denominator has been cancelled out. In practice formula (22) is simplified to the form

$$I=\sum_i\sum_j{}'Z_iZ_j\frac{\sin sr_{ij}}{sr_{ij}}=Z_{Cl}^2\frac{12\sin 2.87s}{2.87s}+Z_CZ_{Cl}\frac{8\sin 1.76s}{1.76s}. \qquad (23)$$

The prime on the double summation indicates that the constant terms corresponding to $i=j$ (which are just Z_i^2) have been neglected. (23) follows immediately from (22) (except for an unimportant constant factor) if the incoherent scattering is a small part of the atomic background and if $(Z-F)_i/Z_i$ is constant for all atoms. It is emphasized that this approximate derivation of (23) makes no prediction concerning the accuracy of the results of its application;

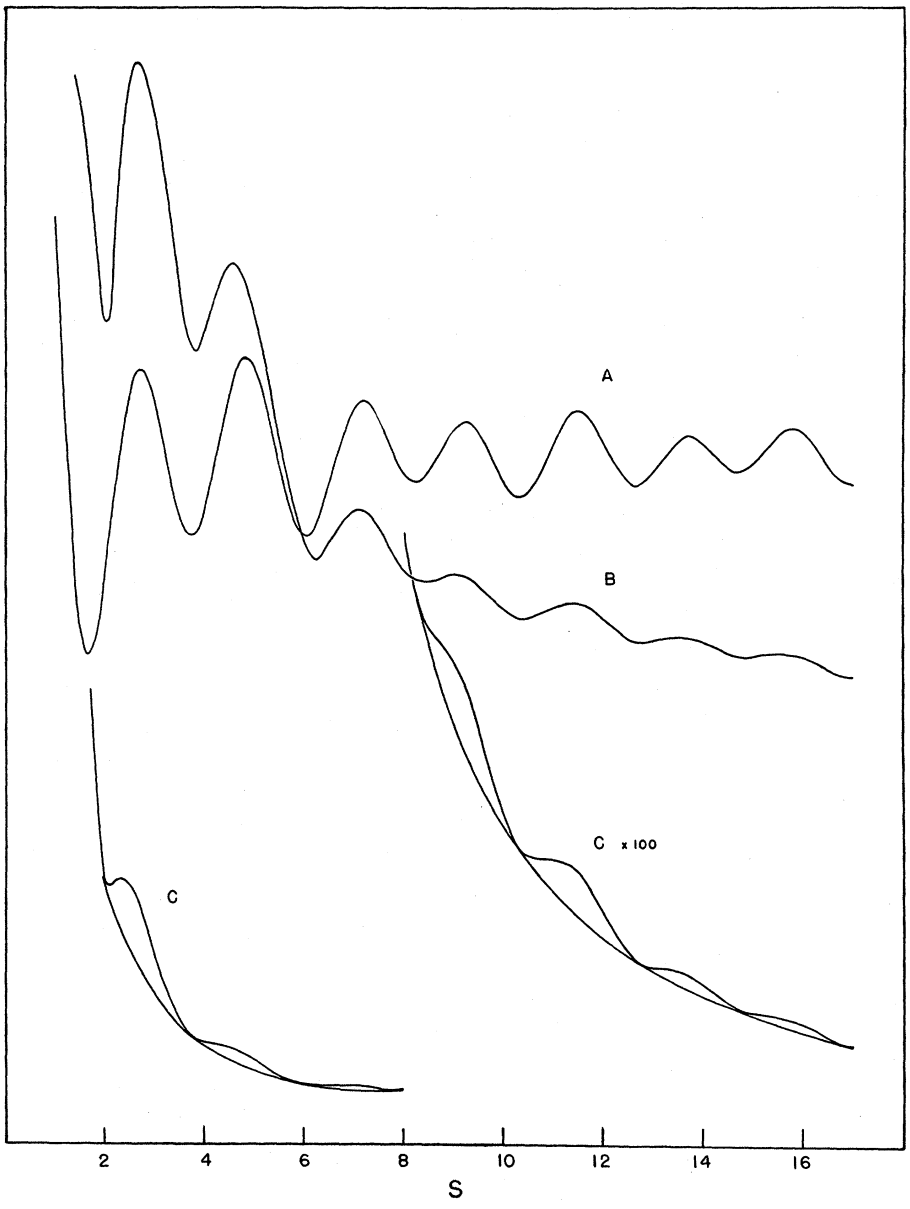

FIG. 9. Theoretical electron diffraction curves for CCl_4, illustrating various procedures for choosing the points by which theory and experiment are correlated.

that is to be determined by empirical tests.

The curve calculated from formula (23) for CCl_4 is designated as A in Fig. 9. The positions of the maxima and minima differ by less than 0.2 percent after the first two maxima from those given by formula (22). Curve A is like the molecular scattering curve, I_3 in Fig. 7, except for the disappearance of the strong damping effect due to the substitution of Z_i for f_i. Curve A reproduces the qualitative features of the photograph in that the fourth and sixth maxima fall below the fifth and seventh, respectively, although it does not show the decrease with increasing angle observed in the photographs.

For the correlation the theoretical points are read from the curve. The experimental points are determined from the measured diameters of the visual maxima and minima. The original negative is illuminated in some standard way and for a given ring the separation, along a diameter, of the two points of greatest apparent density is measured. This is perhaps best done with the aid of a device which holds the film on an illuminated plate and which has two pointers mounted on carriages having independent transverse micrometer motions. The measured diameters are then converted to a set of observed s values which are compared with the calculated s values. Table II taken from Brockway and Wall[38] shows such a comparison for CCl_4.

TABLE II. *Carbon tetrachloride. Camera distance* = 12.19 cm, $\lambda = 0.0604$ to 0.0619A.

No. of Photos	Max.	Min.	s(calc.)	s(obs.)	C−Cl
13	1		2.73	2.870	(1.675)
19		2	3.65	3.789	(1.697)
19	2		4.82	4.912	(1.727)
19		3	6.04	6.064	1.752
19	3		7.16	7.144	1.764
19		4	8.22	8.224	1.759
19	4		9.22	9.263	1.751
19		5	10.27	10.33	1.752
19	5		11.48	11.44	1.765
16		6	12.64	12.58	1.767
16	6		13.69	13.65	1.765
10		7	14.71	14.71	1.760
10	7		15.76	15.81	1.756
4		8	16.92	16.89	1.764
4	8		18.10	18.02	1.768
2		9	19.18	19.07	1.771
2	9		20.18	20.14	1.763
1		10	21.17	21.22	1.756
1	10		22.37	22.34	1.762
				Weighted Average	1.760

The ratio of the calculated to the observed s values applied to the interatomic distance assumed in the formula gives the interatomic distance as determined by the photographs. The values in the last column of Table II are equal to $(s(\text{calc.})/s(\text{obs.}))\cdot 1.76$ for each ring. The distance 1.76A was assumed for convenience in making the theoretical calculations but the use of any other value would not affect the observed distances listed in Table II. The small deviations among these values from the different rings lends support to the method of correlation used. Sources of error in the mean value are discussed below.

In general several molecular models will have to be tested in this way since the comparison described yields a direct determination of the size of the molecule but not of its shape. Different sets of assumed interatomic distances corresponding to variations in the molecular configuration are used in the calculation of curves for several models. A choice can usually be made among these models by requiring the theoretical curve to reproduce the qualitative features observed in the photographs. A ring which is observed to be stronger or weaker than both of its neighbors will show the same effect in the correct theoretical curve. This is also true of a doublet (or two close-lying rings), a ring with a shelf, a ring which shows a sharp fall in apparent density on one side and a gradual fall on the other, etc. A model which yields a consistent set of interatomic distance values calculated according to the foregoing paragraph must also show qualitative agreement with the photographs in order to be accepted as the correct model. In this way some account is taken of the intensity distribution in addition to the matching of a number of isolated points. This criterion for the choice of model is very useful and represents one of the advantages of the visual method since this treatment is based chiefly on the molecular scattering.

Subjective errors in measuring the photographs are found in setting on a point of maximum apparent density when the brightness in the background of transmitted light is much different on the two sides of the point. This effect was first investigated by St. John and Ware[39] who measured asymmetric spectral lines

with a recording microphotometer and a filar micrometer and found that in subjective measurements the maximum was always shifted toward the side of greater contrast. In the measurement of a doublet the apparent separation is greater than the true. The St. John effect is observed in the measurement of electron diffraction photographs. The measurements of asymmetric rings of the sort mentioned above as distinctive qualitative features lead to values of the interatomic distances which may differ by several percent from the value determined from the sharp, well-defined rings. The interatomic distance is too large in the case of a ring with a shelf or shoulder on the outer side (in the direction of greater scattering angle) and too small when the shelf is on the inner side. In the case of SF_6[40] a close double ring was found whose components were shifted in opposite directions by nearly equal amounts as determined by measurements on sharp single rings lying farther out. Although these asymmetric features are valuable in choosing molecular models they cannot give good quantitative agreement in the distances; and since the amount of the correction cannot be predicted the values from these rings are to be discarded in arriving at the final value for the size of the molecule.

An error is usually observed in the measurement of the first two or three rings as illustrated in Table II. This is undoubtedly due to the very rapid increase in intensity as the central image is approached. The background is much steeper here than in the outer part of the pattern and the St. John effect would shift the apparent points of maximum blackening toward larger s values. That the effect is not entirely subjective has been demonstrated by Cosslett[41] who observes a similar effect on microphotometer records. His method of compensating for the steep background is described in the latter part of this section. He attributes the effect to an approach to saturation of the photographic emulsion but some of the subjective error persists in lightly exposed negatives in which the central portion of the photograph is very probably light enough to fall on the linear portion of the characteristic curve. Some of the effect may be due to contrast effects of the very dense central image itself. Cosslett has also suggested the use of positive films for visual measurements but this will not be generally applicable because of the difficulty of printing the light outer part of the pattern. The errors around the central image have no serious consequence in the determination of the structure whenever a fair number of outer rings can be measured.

Since a very large number of curves need to be calculated in the study of a series of chemical compounds it is desirable that the calculations shall be as simple as possible. In this respect the visual treatment is superior to all others since it does not require the use of F-factors. The formulae used are of the general type,

$$I=\sum_i A_i(\sin a_i x)/a_i x, \tag{24}$$

where A_i and a_i are constants. Sherman's table of $(\sin x)/x$[42] was prepared for electron diffraction calculations. More recently tables[43] of $(\sin ax)/ax$ have been printed on long strips of paper; the strips with the appropriate a-values are selected and mounted side by side, and the multiplication by the constants A_i and the summation are performed in one continuous operation on a calculating machine. A formula like (24) involving ten or more terms can be calculated out to $s=20$ in steps of 0.2 in three or four hours.

The accuracy of the visual method has been specifically tested by comparison of its results on the diatomic molecules, chlorine, bromine, and iodine monochloride with the results of the rotational analysis of the absorption spectra of the same compounds.[37] The deviations in the electron diffraction interatomic distances are $+1.1$, $+0.4$, and -0.6 percent, respectively. A discussion of the sources of error is given below.

The particular advantages of the visual method lie in the simplicity of its application, the extensive use which it makes of the qualitative intensity relations over appreciable ranges of scattering angle and the greater number of maxima and minima which are used than in any other method. The first advantage is practically essential in the study of large numbers of substances. The second lends confidence in the choice of models. The third increases the number of independent determinations of the molecular size as well as supporting the choice of model since the outer rings are more sensitive to

changes in model than are the inner rings. The visual method has the disadvantage that possible subjective errors in measurement have to be treated with some care.

Bauer[118] has proposed an analytical procedure for correlating the visual measurements with the theoretical intensity curve given by Eq. (23). The visually measured rings are matched with the corresponding maxima and minima in the curve of Eq. (23) with the aid of the following analytical expression for the positions of the maxima and minima:

$$\sum_{ij} Z_i Z_j (\cos s_k r_{ij} - (\sin s_k r_{ij})/s_k r_{ij}) = 0, \qquad (24a)$$

in which s_k is the observed s value for the k^{th} ring. If the correct model has been chosen each of the k expressions represented by (24a) will be equal to zero; in general these equations will lead to a set of residuals. Bauer has shown how to obtain the corrections to be applied to the assumed values of the r_{ij}'s and thereby obtain a set of interatomic distances which will satisfy (24a).

This procedure should be useful when the photographs show a large number of sharp, well-defined rings and for such cases it may be carried through with less work than is required by the treatment described above. On the other hand the use of the qualitative appearance of the photographs (asymmetric rings, relative intensities, etc.) in choosing the molecular model is not possible in the analytical procedure. The errors in measurement introduced by the St. John effect require certain rings to be entirely ignored. These limitations are serious enough so that the analytical procedure will not be generally useful until more complete diffraction patterns are obtained.

Microphotometer method

The other principal method of interpreting electron diffraction photographs consists of the correlation of points on the complete theoretical intensity curve with points on microphotometer records. The complete curve is calculated for the model to be tested and plotted as in C of Fig. 9. A smooth background curve without fluctuations is then drawn so that it is tangent to the intensity curve on the lower side. The points for correlation have been chosen in three different ways. Maxwell, Hendricks, and Mosley[44] select the positions of the vertical lines which bisect the areas enclosed between the smooth background and the intensity curve. Cosslett[41] and others have chosen the points on the intensity curve lying highest above the background in each of the areas. Brockway and Pauling[37] used the tangent points themselves. Of these procedures the first is probably least subject to uncertainties due to variations in the manner of drawing in the background although the uncertainties are small in any case. These same procedures could be applied to a second tangent curve drawn on top of the intensity curve; for the first two this would be analogous to the measurement of the minima in the visual treatment. Degard and van der Grinten[45] use the atomic scattering curve (including coherent and incoherent scattering, i.e., I_1 and I_2) for the smooth background. This crosses the complete intensity curve at the points of inflection and these points are used by the authors for the correlation with the analogous points on the microphotometer curve.

TABLE III. *Comparison of correlating points on theoretical CCl_4 curves.*

MAX.	s^2	I_4 AREA BISECTED	I_4 HIGHEST POINT	$I_4 \cdot s^2$
1	2.73	2.65	2.6	2.65
2	4.82	4.70	4.6	4.56
3	7.16	7.12	7.1	7.15
4	9.22	9.18	9.2	9.10
5	11.48	11.47	11.5	11.5
6	13.70	13.66	13.7	13.6
7	15.76	15.75	15.8	15.6

In Table III a comparison is made of the correlating points for CCl_4 obtained from the theoretical "visual" curve and by the first two methods of the preceding paragraph. Beyond the second "maximum" the differences are insignificant; for the first two the visual points are several percent larger. It has been claimed that this comparison indicates a lesser accuracy of the results of the visual method. This could be true only if the same experimental points were correlated with these different theoretical points; in practice each treatment of the theoretical intensity is matched with a corresponding experimental treatment and the accuracy of the results of the various procedures is to be tested by empirical comparisons with molecular structures known from entirely different experiments. The error which is observed in the results obtained from the first one or two rings cannot be explained by the larger size of the s values for the theoretical points since the error is in the opposite direction.

The experimental points for the methods described above were chosen on the microphotometer records by the same respective procedures, and comparisons of observed and theo-

retical s values were carried out in the same way as in the visual treatment illustrated in Table II. Although there may be some differences between the microphotometer records and the curve representing experimental electron intensities these differences would not be expected to have an appreciable effect on the s values of the points chosen by the described procedures. Maxwell, Hendricks, and Mosley[44] have tested this effect in photographs of 4, 4′-diiododiphenyl ether and phosphorus (P_4). They calibrated the photographic emulsion with a series of test spots of different exposure times. Points corresponding to the positions of the vertical bisectors of the areas between the smooth background and the experimental intensity curve were found to agree with the points obtained from the microphotometer curve. No correction was made for the experimental background due to multiple scattering, scattering by gas molecules all along the path of the electron beam, etc., but this is unimportant except for quantitative intensity comparisons.

The background of inelastic scattering has not always been included in the theoretical curves. This background has an effect in the region of small s values where it is a large part of the total scattering and is falling very rapidly. Farther out it has a negligible effect on the points chosen as above. Whether this background should be included depends on the region in which the measurements are to be made.

The consideration of various molecular models is to be carried out for the reasons discussed under the visual method but unless the changes in molecular configuration are accompanied by appreciable changes in the s-scale of the molecular scattering curve (I_3 in Fig. 7), the complete theoretical curve will not be much affected. Changes in the relative amplitude of the humps on the molecular scattering curve appear on a relatively smaller scale in the fluctuations of the complete curve, and methods involving the use of complete theoretical curves are somewhat less sensitive to small changes in the molecular configuration than is the visual method.

The accuracy of the methods is indicated by the interatomic separation of 2.65A obtained for iodine molecule[46] (band spectral value-2.66A) and by the general agreement with the results of the more thoroughly tested visual method. The use of complete theoretical curves and microphotometer records has the advantage of escaping the subjective errors of the visual method. It generally treats a smaller number of points than the visual method since the light outer part of the diffraction pattern is not registered by the microphotometer, and this part of the curve is affected most by small changes in molecular configuration. A serious disadvantage when a large number of substances are to be studied is the laborious calculations involved in this method compared to the simpler theory and calculations of the visual method.

"Compensation" methods

Other procedures have been used in which various means of compensating for the very rapid fall in intensity are used. The most generally useful of these was proposed by Maxwell, Hendricks, and Mosley[44] who multiplied the theoretical and experimental intensity curves (the latter obtained from calibrated densitometer methods) by s^2. Such a curve for CCl_4 is shown in Fig. 9-*B*. The multiplying factor converts the fluctuations into real maxima and minima and the resulting curve is similar to that used in the visual treatment (Fig. 9-*A*). Curve *B* shows the gradual decrease in the background intensity which appears in the photographs but it exaggerates the prominence of the inner maxima relative to the outer ones. The theoretical and experimental points which are correlated are the positions of the maxima and minima on the respective curves of $s^2 \times I$. These values for CCl_4 are included in the last column of Table III. This method leads to essentially the same interatomic distance results obtained by the direct use of microphotometer records.

A different procedure was used by Cosslett[41] in studying the deviations observed in the first two rings of CCl_4. He prepared a compensating plate whose density distribution represented the complement of the smooth background along a radius of the original electron diffraction negative. This he did by taking a microphotometer record of the original negative, drawing in the smooth background, preparing a cell of absorbing liquid with the same shape as the background

curve and exposing a photographic plate to light passing through the cell. The negative and the compensating plate were laid together and a third plate was exposed through the two. The compensated plate thus obtained was a positive of the deviations of the intensity curve from the smooth background. This was photometered and the record showed pronounced minima at the positions of the "maxima" in the original plate. These points were correlated with theoretical points corresponding to maximum height of the theoretical intensity curve above its smooth background. The resulting interatomic distances were in excellent agreement with those obtained from the outer rings by the usual treatment of microphotometer records. Cosslett's method is applicable only to the steepest part of the intensity curve but it is here that the correction is necessary. He ascribed the error found in the ordinary treatment of these rings to the saturation of the photographic emulsion due to the very high intensities near the central beam.

Another compensation method developed by Trendelenburg[47] makes use of a rotating sector in preparing copies of the original negative. The sector is graduated to compensate for the background but the relative intensities of the rings are changed. This procedure has been applied on powder photographs but not on the diffraction patterns of gases.

The contrast microphotometer constructed by Sears[48] has been used on electron diffraction photographs. In this instrument the negative is moved across the image of a microphotometer slit with an oscillation parallel to the direction of travel in addition to the steady translation. The transmitted light falls on a photo-cell and the photoelectric current is taken through an a.c. amplifier and registered on a current measuring device. The instrument registers density gradient rather than density and hence is sensitive to changes in the curvature of the intensity curve. This density gradient curve may be matched with a curve showing the first derivative of the theoretical intensity or it may be used to locate characteristic points on the intensity curve (especially points of inflection) and the latter procedure has been applied to photographs of benzene and carbon tetrachloride with satisfactory results.

Radial distribution method

All of the methods of interpreting the photographs of gases described above consist in testing preconceived models of the structure of the molecule. The radial distribution method described by Pauling and Brockway[49] offers the important advantage of yielding information about the structure without making any assumptions or using previous knowledge. From the data of the electron diffraction photographs a distribution function for scattering power is calculated which represents the product of scattering powers in volume elements the distance r apart as a function of r. Since the electrons are scattered mainly by the atomic nuclei a maximum in this function represents an internuclear distance in the molecule equal to the corresponding value of r. In this way the radial distribution method leads directly to the interatomic distances and the structure of the molecule.

The theoretical intensity given by formula (17) is

$$I(s)=K\sum_i\sum_j f_i f_j\,(\sin sr_{ij})/sr_{ij}. \qquad (25)$$

In deriving this expression it was assumed that the scatterer is a molecule consisting of discrete atoms and the summations are carried over the atoms. The f-factors include integrals arising from the continuous distribution of scattering power within the atoms. A more general expression is obtained if the molecule as a whole is treated as having a continuous distribution of scattering power. In place of (25) we have

$$I(s)=K'\int_0^\infty (r^2D(r)/s^4)((\sin sr)/sr)dr. \qquad (26)$$

The summation has been replaced by the integral over dr and the product of atomic scattering factors is replaced by the function $r^2D(r)/s^4$ in which $r^2D(r)$ represents the product of scattering powers in all volume elements the distance r apart. On writing (26) in the form

$$s^5I(s)=K'\int_0^\infty rD(r)\sin srdr$$

it is evident that the integral may be inverted

to give

$$rD(r)=K''\int_0^\infty s^5 I(s)\sin srds$$

or

$$D(r)=K''\int_0^\infty s^6 I(s)((\sin sr)/sr)ds. \qquad (27)$$

The integral could be evaluated if quantitative experimental intensities were measured. It is more useful, however, to replace the integral by a summation

$$D(r)=\sum_k I_k(\sin s_k r)/s_k r, \qquad (28)$$

in which one term appears for each ring observed on the diffraction photograph. s_k is the s value for the kth ring (determined for this application by the visual method) and I_k is a visually estimated value of the intensity of the kth ring. $D(r)$ is then calculated with the aid of the $(\sin ax)/ax$ tables mentioned above.

The applicability of formula (28) is discussed in detail in the original reference. It is found that the positions of the maxima in $D(r)$ are only slightly affected by changes in the estimated intensities so that the interatomic distances are determined mainly by the observed ring diameters. The method was tested on chlorine and bromine and on more complicated molecules in which the geometry of the molecule determines the ratio of the interatomic distances (such as benzene, carbon disulfide, etc.). In general the most prominent maximum in $D(r)$ yields a value for the interatomic distance which is accurate to about one percent; other peaks yield less accurate values. The radial distribution function for CCl_4 from ten observed maxima is reproduced in Fig. 10. The sharp maximum at 2.86A is the Cl—Cl distance which has the same value when determined by the usual method. The smaller peak corresponds to the C—Cl distance with a value of 1.74A; this is 0.01A or more too small. Beyond about 3.5A the curve has no meaning; if the integral of (26) had been used the curve would fall asymptotically to zero in this region.

The direct information afforded by the radial distribution method is very useful but frequently does not lead to a complete structure determination because of the small number of interatomic distances for which accurate values are obtained. Also when slightly differing distances occur in the molecule they may not be resolved in the distribution function. On the other hand, the application of the method immediately limits the range of parameter values to be investigated. It also affords a superior treatment for molecules containing rotating groups of atoms and for molecules in which the choice of the model depends on quantitative intensity estimates (ClO_2, SO_2, etc.).

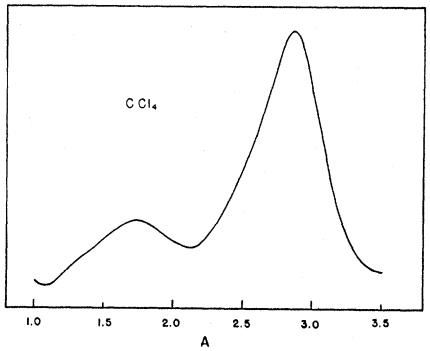

FIG. 10. Radial distribution function for CCl_4.

Determination of molecular structure

The general procedure for attacking structure problems and the types of structure which can be determined may be reviewed briefly before the reliability of the results is discussed. After the photographs are obtained, the first step recommended is the calculation of the radial distribution function by use of visual measurements of $s(=(4\pi \sin \theta/2)/\lambda)$ and of visually estimated intensities. Then theoretical intensity curves are calculated in order to test the models which are compatible with the results of the radial distribution method. The most accurate means of doing this is the matching of experimental and theoretical intensities over a continuous range of the angle variable s (as described above for benzene) but the general shape of the intensity curves and the labor involved limits the applicability of this method. A choice is to be made then among the methods which correlate individual points of the theoretical and experimental diffraction patterns; and these are divided into the visual method and the microphotometer methods. The measurement

of interatomic distance from a single ring is about equally accurate by the two procedures. Values from the innermost rings are too small in both cases (except for the compensating treatment suggested for the microphotometer method by Cosslett). The visual measurements of certain rings are influenced by subjective errors (St. John effect) but these are easily recognized; and such measurements which are discarded in determining the most probable value of the interatomic separation are never a large part of the total number of measurements on a compound. Whenever the molecular configuration is known from other data or the variations to be tested involve changes in the separations of the heavier atoms in the molecule the two procedures have about the same accuracy. The visual method allows a greater number of points to be correlated since the eye registers more rings than the microphotometer does; moreoever, the outer part of the pattern is more sensitive than the inner part to changes in molecular configuration. In general, for the determination of configuration parameters the visual method is to be preferred.

Simplicity of application also favors the visual method. The more involved calculations of the theoretical intensity in the microphotometer method are not repaid by an increase in accuracy of the result; and they decrease the number of models which it is practical to treat in the study of a series of compounds.

Some investigators have raised the question of which of all the methods of treating the photographs is "justifiable." If a complete quantitative test of the theoretical intensity of electron scattering is desired none of the foregoing treatments is justifiable. If molecular configuration and size is to be determined by the correlation of s values of a few characteristic points on the theoretical curves and the photographs, a justifiable procedure will be any which gives a consistent treatment to theory and experiment (i.e., which matches theoretical "visual" curves with visual measurements or complete theoretical curves with experimental intensity curves) and more particularly a procedure which is sensitive to changes in molecular model and which gives accurate results. In any event it is highly important that an investigator choose and adhere to specified ways of treating theory and photographs and that he test his own application of the experiment by investigating compounds whose structures are known.

The stochastic nature of the electron diffraction treatment (excepting the radial distribution method) is not always recognized. Excellent agreement between the photographs and the intensity curve for a particular model of a molecule does not constitute a unique determination of the structure. Other values of the configuration parameters are possible unless they are specifically eliminated by treatment of the corresponding intensity curves. It is always desirable to limit the uncertainties in the configuration parameters by testing a series of molecular models until definite disagreement with the photographs is found and unless this is done the configuration of the molecule has not been determined. It is permissible and often necessary to assume some of the parameter values which have been determined by other methods; but assumed parameter values are not determined by the electron diffraction results. The assumed values are merely shown to be compatible with the results of the experiment. In this respect an investigator should not be satisfied with only rough agreement between theory and experiment; changes in the parameters may lead to definite improvement in the agreement and hence to an actual determination of parameter values. The report of the results is incomplete without a list of the various molecular models tested showing which interatomic distances or bond angles were assumed and which were determined.

An illustration of the use of assumed parameter values may be given for the benzene molecule (regarding only the six carbon atoms, for convenience). If the six carbon atoms were put in perfectly general positions the variables to be treated would be too numerous. One does not hesitate to accept the chemical evidence and to assume that the six carbon atoms form a ring and that the carbon-carbon bonds are equivalent. This leaves only two parameters; one determines the configuration (i.e., whether the ring is staggered or plane) and the other fixes the size of the ring or the bond distances. As a part of the investigation referred to above[14] the configuration parameter was determined by means of three models in which the two planes contain-

ing the sets of three alternating carbon atoms were separated by 0.2, 0.1, and 0.0A, respectively. After the latter was shown to be the most nearly correct representation of the molecule the size was determined by matching the scale of the experimental and theoretical curves.

Certain types of structure cannot be determined completely. Examples of one of these types are ClO_2[50] and SO_2.[10, 51] Here the central atom of the triatomic molecule has a much greater scattering power than the outer atoms. As a consequence the two Cl−O (or S−O) interference terms chiefly determine the diffraction pattern and the effect of changing the O−O term accompanying the variation of the bond angle from 60° to 180° is scarcely detectable in the theoretical intensity curve. Even with the radial distribution method only an approximate determination of the angle was made but this uncertainty does not affect the determination of the Cl−O distance. In general molecules which contain some light and some heavy atoms (i.e., differing by a factor of two or more in atomic number) cannot have the distances between the light atoms determined with any accuracy. This limitation makes it impossible to locate hydrogen atoms. Although hydrogen atoms cannot be neglected in calculating scattering curves, relatively large changes in their positions have a very slight effect on the curves. Whenever the number of atoms in the molecule is large a complete structure determination is not possible by electron diffraction methods because the probability of the existence of different sets of parameter values leading to the same theoretical intensity is too great. The determination of more than three parameters (including the size of the molecule) is not feasible but the use of electron diffraction methods in conjunction with other data has made it possible to study many complicated molecules.

Sources of error

The probable error in electron diffraction results depends on a number of factors; in favorable cases it may be as little as one percent or even less. The scale of distances is fixed by the value 4.070A taken for the edge of the unit cell in gold (Neuberger's[29] value for 1936 is 4.0700 ±0.0004A referred to the Siegbahn scale). The de Broglie wave-length as calibrated by gold foil in this laboratory shows an average deviation from the mean of the measurements of the rings on a single photograph of about 0.3 percent; with good voltage control and recalibration at regular intervals the uncertainty in the wave-length is not more than 0.5 percent. Errors in the measurement of the scattering angle θ have relative and not absolute significance since the validity of the point which is chosen to be measured is determined by an empirical test on the interatomic distance result. Repeated measurements on the diameter of a sharp ring by the visual method using pointers with micrometer movements can be made with a maximum deviation of about 0.5 percent. Measurements on poorly defined rings showing fluctuations as large as 2 percent are generally discarded as unreliable. The uncertainty in the camera distance, which lies between 100 and 300 millimeters, is easily kept below 0.5 percent. In general the probable error in the $(\sin \theta/2)/\lambda$ values as measured for the chosen points on the photograph is safely estimated at about one percent. The theoretical s values for a given molecular model may be determined as accurately as desired by calculating the corresponding intensity function at small enough intervals of the argument to fix the position of the curve within very narrow limits. In the correlation of theory and experiment the consistency of the values of the interatomic distance determined by the different rings (with due allowance for known causes of fluctuations) is a measure of the reliability of the result. The average deviation from the mean of these values varies from $\frac{3}{4}$ percent for CCl_4 (including the uncertainty in wave-length due to voltage fluctuations) to 5 percent or more for ethylene and other molecules of very low scattering power. The probable error, which is less than this average deviation, lies between one and two percent for most substances which have been studied; this estimate is supported by the comparison with the results of band spectral investigations mentioned above.

The foregoing discussion applies to the determination of molecular size. If the configuration is uncertain the error can be fixed only by finding the limits on the variation of the configuration parameters which cause definite dis-

agreement of the corresponding intensity curves with the photographs. The limits of the uncertainty depend entirely on the character of the substance being studied as was pointed out in the discussion on choice of molecular models.

Another possible source of error is the existence of impurities in the sample of the substance under investigation. If the nature and amount of the impurity is known its effect may be tested by calculating electron scattering curves for both substance and impurity and averaging the two curves according to the relative molecular concentrations. If the impurity has a molecular scattering power no greater than that of the substance, concentrations of the order of one percent will have no effect.

Electron and x-ray diffraction results on CCl_4

The only generally applicable methods of determining interatomic distances are electron and x-ray diffraction. A comparison of the merits of electron and x-ray diffraction leads to the conclusion that each has its own field. In crystal structure investigations, x-rays are superior because of their greater penetrating power; electrons on the other hand are very useful in the study of the surface structure of solids. In diffraction by gas molecules electron beams are superior in locating atomic positions because they are scattered mainly by the atomic nuclei whereas x-rays are scattered by the atomic electrons which especially for the light atoms are more or less concentrated in the bonds. Bewilogua[52] has given this comparison in detail.

A brief history of the study of CCl_4 by the two methods is given here because of the importance of this substance in its extensive use in standardizing experimental procedures in electron diffraction, and because of the discrepancy which existed in the results of the two methods. The molecule has always been treated as a regular tetrahedron with the chlorine atoms at the four apices and the carbon atom at the center. The size is reported here in terms of the C−Cl bond distance; the Cl−Cl separation is obtained by applying the factor $(8/3)^{\frac{1}{2}}(=1.633)$.

In 1929 the first x-ray value of 2.0A was reported by Debye, Bewilogua, and F. Ehrhardt.[53] A short time later a more complete theory of x-ray scattering by gas molecules led to the value of 1.9A[54] and finally to the 1930 value of 1.83 ±0.02A.[55] In 1933 van der Grinten[27] confirmed the 1930 value. The first electron diffraction value of the C−Cl distance in CCl_4 was 1.81A reported by Wierl[56] in 1930. In succeeding years various investigators using electron diffraction

TABLE IV.

Compound	Structure type	Configuration	Bond distance (A)		References
Inorganic Molecules					
Second Group					
$HgCl_2$	$3-D_{\infty h}$	Linear	2.28(±0.05)		63
$HgBr_2$	$3-D_{\infty h}$	Linear	2.38(±0.05)		63
HgI_2	$3-D_{\infty h}$	Linear	2.55(±0.05)		63
Third Group					
$B_3N_3H_6$	$12-D_{3h}$	Reg. hexagonal	1.47±0.07 (B−N)		109
BCl_3	$4-D_{3h}$	Planar	1.73±0.02		74, 112, 113
BBr_3	$4-D_{3h}$	Planar	1.87±0.02		74
TlCl	$2-C_{\infty v}$		2.55±0.03		92
TlBr	$2-C_{\infty v}$		2.68±0.03		92
TlI	$2-C_{\infty v}$		2.87±0.03		92
Fourth Group					
SiF_4	$5-T_d$	Tetrahedral	1.54±0.02		78, 106
$SiHCl_3$	$5-C_{3v}$		2.00±0.03	110°±3°	75
$SiCl_4$	$5-T_d$	Tetrahedral	2.00±0.02		65, 78, 106, 112, 115
$TiCl_4$	$5-T_d$	Tetrahedral	2.21±0.05		112, 115
$GeCl_4$	$5-T_d$	Tetrahedral	2.08±0.03		66, 106, 112, 115
$SnCl_4$	$5-T_d$	Tetrahedral	2.30±0.03		78, 106, 112
Fifth Group					
N_2O	$3-C_{\infty v}$	Linear	2.38±0.05 between end atoms		104, 112, 113
NO_2	$3-C_{2v}$	Bent			104
N_2O_4					104
N_2O_5					104
P_4	$4-T_d$	Tetrahedral	2.21±0.02		103
PF_3	$4-C_{3v}$	Pyramidal	1.52±0.04	104°±4°	78, 106
Fifth Group (continued)					
PF_5			1.57±0.03		70
$PFCl_2$			P−Cl=2.00±0.03		70
PCl_3	$4-C_{3v}$	Pyramidal	2.00±0.02	101°±2°	78, 106, 112, 113
$POCl_3$				104°±4°	70
As_4	$4-T_d$	Tetrahedral	2.44±0.03		103
AsF_3	$4-C_{3v}$	Pyramidal	1.72±0.02	—	78, 106
$AsCl_3$	$4-C_{3v}$	Pyramidal	2.16±0.03	103°±3°	78, 106
Sixth Group					
OF_2	$3-C_{2v}$	Bent	1.41±0.05	100°±3°	60, 61, 110
Cl_2O	$3-C_{2v}$	Bent	1.68±0.03	115°±4°	106, 110
SO_2	$3-C_{2v}$	Bent	1.45±0.02	124°±15°	85, 106, 112, 113
SF_6	$7-O_h$	Octahedral	1.57±0.03		65, 77
S_2Cl_2	S−Cl=1.98±0.05		S−S=2.04±0.05		117
SeF_6	$7-O_h$	Octahedral	1.68±0.03		65, 77
TeF_6	$7-O_h$	Octahedral	1.83±0.03		65, 77
$TeCl_2$		Linear (?)	2.36±0.03	>150°	92
$TeBr_2$		Linear (?)	2.49±0.03	>150°	92
Seventh Group					
Cl_2	$2-D_{\infty h}$		2.01±0.03		108
ClO_2	$3-C_{2v}$	Bent	1.53±0.02	117°±15°	67, 68, 106
Br_2	$2-D_{\infty h}$		2.28±0.02		108, 112, 113
I_2	$2-D_{\infty h}$		2.65±0.10		93
ICl	$2-C_{\infty v}$		2.30±0.03		108
Transition Groups					
OsO_4			1.66±0.05		69
OsF_8	$9-D_{4d}$	Archimedes antiprism (?)	2.52±0.10		64

TABLE IV.—*Continued.*

Compound	Configuration	Bond distance (A)	References
	Organic Molecules		
	Aliphatic Molecules—C_1 Group		
CH_3F		1.42±0.02	73
CF_4	Tetrahedral	1.36±0.02	60, 61, 78, 106
$CHFCl_2$		C−F=1.36±0.02 C−Cl=1.74±0.03	75
CF_2Cl_2		C−F=1.36±0.02 C−Cl=1.75±0.03	75
CH_3Cl		1.77±0.02	110
CH_2Cl_2		1.77±0.02 112°±2°	106, 110, 112
$CHCl_3$		1.77±0.02 112°±2°	106, 110, 112
CCl_4	Tetrahedral	1.755±0.005	65, 78, 83, 84, 87, 88, 91 93, 94, 106, 108, 112, 115
CH_3Br		(2.06±0.05)	90
CH_2Br_2		1.91±0.03 112°±2°	74, 90
$CHBr_3$		(2.03±0.05)	90, 111
CBr_4	Tetrahedral	1.93(±0.03)	96, 112
CH_3I		(2.28±0.05)	90
CH_2I_2		(2.28±0.05)	90
CHI_3		2.12(±0.03)	96
$COCl_2$	Planar	C−O=1.28±0.02, ∠ClCCl=117°±2° C−Cl=1.68±0.02	71, 89
$COBr_2$	Planar	(C−O=1.13, C−Br=2.05±0.04)	89
$CSCl_2$	Planar	C−S=1.63, ∠ClCCl=116° C−Cl=1.70±0.02	71
CH_2O	Planar	(C−O=1.15±0.05)	81
CO_2	Linear	1.13±0.04	112, 113
CH_3ONH_2	Bent	C−O=1.44±0.02, 111°±3° N−O=1.37±0.02	71
CH_3NO_2	Planar	C−N=1.46±0.02, ∠ONO=127°±3° N−O=1.21±0.02	71
COS	Linear	C−O=1.16±0.03, C−S=1.56±0.04	60, 61, 85, 89
CH_2N_2	Linear	C−N=1.34±0.05, N−N=1.13±0.04	60, 61
CH_3N_3		C−N_1=1.47±0.02, N_1−N_2=1.26±0.02 N_2−N_3=1.10±0.02, ∠CN$_1$N$_2$=120°±5°	76, 105
CS_2	Linear	1.54±0.03	85, 112, 113

Compound	Configuration	Bond distance (A)		References
	Organic Molecules			
	Aliphatic Molecules—C_2 Group			
		C−C (A)	C−X (A)	
Ethane Derivatives				
C_2H_6		1.52±0.1		111
C_2H_5Cl			1.81±0.1	80
$C_2H_4Cl_2$ (1, 1−)			Cl−Cl=2.9±0.3	111, 116
$C_2H_4Cl_2$ (1, 2)				111, 116
C_2H_5Br			(2.02±0.07)	80
$C_2H_4Br_2$ (1, 1)			Br−Br=3.56±0.15	111
$C_2H_4Br_2$ (1, 2)			Br−Br=4.75±0.15	111
C_2H_5I			(2.32±0.05)	80
CH_3CHO		1.51±0.05	C−O=1.20±0.05 LCCO=122°	117
CH_3COCl		1.54	(C−O=1.14±0.05) (C−Cl=1.82±0.10)	89
$(COCl)_2$				116
CH_3COBr		1.54	(C−O=1.13±0.05) (C−Br=2.06±0.10)	89
C_2H_4O (ethylene oxide)		1.49±0.1	C−O=1.49±0.1	111, 117
Ethylene Derivatives			LCCX	
C_2H_4		1.3±0.1		111
C_2H_3Cl		1.38	1.69±0.02 122°±2°	71
$C_2H_2Cl_2$ (1, 1)		1.38	1.69±0.02 122°±1°	71, 111
$C_2H_2Cl_2$ (cis)		1.38	1.67±0.03 123.5±1°	71, 111, 116
$C_2H_2Cl_2$ (trans)		1.38	1.69±0.02 122.5±1°	71, 96, 111, 116
C_2HCl_3		1.38	1.71±0.03 123°±2°	71, 91
C_2Cl_4		1.38	1.73±0.02 123.75°±1°	71, 91, 96
C_2H_3Br		(1.32±0.08)	(2.05±0.08)	91
$C_2H_2Br_2$ (cis)		(1.32±0.08)	(2.05±0.08)	91
$C_2H_2Br_2$ (trans)			1.91(±0.05)	91, 96
C_2HBr_3		(1.32±0.08)	(2.05±0.08)	91
C_2Br_4			1.91(±0.05)	96
$C_2H_2I_2$ (trans)			2.10(±0.05)	96
C_2I_4			2.10(±0.05)	96
Acetylene Derivatives				
C_2H_2		1.22±0.1		111
C_2Br_2		1.20±0.03	1.80±0.03	74, 96
C_2I_2		1.18	2.03(±0.05)	96

Compound	Configuration	Bond distance (A)	References
	Aliphatic Molecules—C_2 Group (continued)		
Miscellaneous			
$(CH_3)_2O$		C−O=1.42±0.03 ∠COC=111°±4°	81, 106, 110
$(HCOOH)_2$	Planar	C−O=1.29±0.02 OHO=2.67±0.04 ∠OCO=125°±5°	94, 107
CH_3NNCH_3	Planar	C−N=1.47±0.06 N−N=1.24±0.05 ∠CNN=110°±10°	60, 61
$(CN)_2$	Linear	C−C=1.43±0.03 C−N=1.16±0.02	67, 111
CH_3CN	Linear	C−C=1.55±0.02 C−N=1.16±0.02	69
CH_3NC	Linear	H_3C−N=1.48±0.03 N−C=1.17±0.02	69
$S(CH_3)_2$	Bent	C−S=1.82±0.03	73
	Aliphatic Molecules—C_3 Group		
C_3H_8		C−C=1.52±0.05	111, 118
C_3H_6 (cyclopropane)		1.53±0.02	69, 111
C_3H_4 (allene)		C−C=1.31±0.05	111
$(CH_3)_2CO$		C−C=1.57±0.04	94
C_3O_2	Linear	C−C=1.29±0.03 C−O=1.20±0.02	60, 61, 62, 76
$N(CH_3)_3$		C−N=1.47±0.02	73
	Aliphatic Molecules—C_4 Group		
C_4H_{10}		C−C=1.51±0.05	111
C_4H_8 (trans 2-butene)		C−C=1.53±0.02	69
C_4H_8 (cis 2-butene)		C−C=1.54±0.02	69
C_4H_6 (butadiene)		C−C (single bond)=1.52±0.08	111
C_4H_2 (diacetylene)	Linear	C−C (center)=1.43±0.03 C−C (end)=1.21±0.02	67, 111
C_4H_8O (trans butene oxide)		C−C=1.54±0.02 C−O=1.43±0.02	69
C_4H_8O (cis butene oxide)		C−C=1.53±0.02 C−O=1.42±0.02	69

Compound	Configuration	Bond distance (A)	References
	Aliphatic Molecules—C_4 Group (continued)		
$(C_2H_5)_2O$		(C−O=1.33±0.08)	81
$(C_2H_4O)_2$ (1, 4)		C−C=1.54 C−O=1.46±0.04 ∠COC=110°±5°	110
C_4H_9Br (tert.)		C−C=1.55±0.05 (C−Br=2.06±0.05)	90
$Ni(CO)_4$	Tetrahedral	Ni−C=1.32±0.03 C−O=1.15±0.02	72
$Si(CH_3)_4$		Si−C=1.93±0.03	73
$Ge(CH_3)_4$		Ge−C=1.98±0.03	73
$Sn(CH_3)_4$		Sn−C=2.18±0.03	73
$Pb(CH_3)_4$		Pb−C=2.30±0.05	73
	Aliphatic Molecules—C_5 Group		
C_5H_{12}		C−C=1.53±0.05	111, 112
C_5H_{10} (cyclo)		C−C=1.52±0.03	111, 112
$C(CH_3)_4$		C−C=1.55±0.02	73
	Aliphatic Molecules—C_6 Group		
C_6H_{14}		C−C=1.54±0.05	111, 112
C_6H_{12} (cyclo)		C−C=1.51±0.05	112, 116
$(CH_3-CHO)_3$	Staggered hexagen	C−O=1.43±0.02 C−C=1.54±0.02	82, 117
	Aromatic Molecules	C−C (A)	
C_6H_6	Planar	1.390±0.005	95, 108, 112, 116
C_6Cl_6		1.41 C−Cl=1.69(±0.02)	97
$C_6H_4Br_2$ (1, 4)		1.41 C−Br=1.88(±0.02)	97
$C_6H_3Br_3$ (1, 3, 5)		1.41 C−Br=1.88(±0.02)	97
C_6Br_6		1.41 C−Br=1.88(±0.02)	97
$C_6H_4I_2$ (1, 2)		1.42 C−I=2.00±0.10	93
$C_6H_4I_2$ (1, 3)		1.42 C−I=2.09(±0.10)	93
$C_6H_4I_2$ (1, 4)		1.42 C−I=2.02±0.03	93, 97
$C_6H_3I_3$ (1, 3, 5)		1.41 C−I=2.05(±0.03)	97
$C_6H_4(CH_3)_2$ (1, 4)		1.40±0.01 C−CH_3=1.50±0.01	95
$C_6H_3(CH_3)_3$ (1, 3, 5)		1.40±0.01 C−CH_3=1.50±0.01	95
$C_6(CH_3)_6$		1.40±0.01 C−CH_3=1.50±0.01	95
$(IC_6H_4)_2O$ (4, 4′)		1.42 C−I=2.00, C−O=1.42, ∠C−O−C=118°±3°	103

methods obtained the following values: 1931—Wierl,[112] 1.83A; 1932—Hengstenberg and Bru,[94] 1.83A; 1933—Brockway and Pauling,[77] 1.81A; Braune and Knoke,[65] 1.78A; Dornte,[91] 1.82A; Hendricks, Maxwell, Mosley, and Jefferson,[93] 1.83A; 1934—Pauling and Brockway,[108] 1.76A; Cosslett and de Laszlo,[84] 1.75A; Cosslett,[83] 1.74A; 1935—Degard and van der Grinten,[87, 88] 1.75A; Pauling and Brockway,[106] 1.755A. The earliest electron diffraction results agreed with Bewilogua's x-ray result largely because no independent check had been made on the electron diffraction method. With improvement of the experimental technique and a more careful treatment of the photographs it became apparent that the electron diffraction value was definitely four percent smaller than the x-ray value. A more careful x-ray investigation was carried out in conjunction with the electron diffraction work of Degard, Pierard, and van der Grinten[87] with the result that the x-ray value is now given as 1.75 ± 0.02A.

Two x-ray investigations are of special interest because non-photographic methods of measuring the diffracted rays were used. In 1933 Lu[119] studied several gases including CCl_4 with the aid of an ionization chamber and electrometer; he supported the 1933 value given above (1.83A) with a maximum error of five percent in the observed intensities. Very recently van der Grinten and Brasseur[120] observed the first two diffraction maxima from CCl_4 vapor by means of a Geiger-Müller counter. Their value for the C−Cl distance is 1.73A.

The most probable value of the C−Cl distance in molecules of gaseous carbon tetrachloride is 1.755 ± 0.005A.[106] The care with which this substance has been studied by a number of investigators makes it possible to assign a smaller than the usual probable error.

V. Survey of Results

Electron diffraction methods have been used in studying the molecular structure of a number of compounds. The results have been applied to problems in structural chemistry and a few specific applications will be illustrated here.

The earliest application was made by Wierl[116] to distinguish between the *cis*- and *trans*-forms of 1,2-dichloroethylene. Chemical evidence shows that in each of these compounds two carbon atoms are joined by a double bond with one hydrogen and one chlorine atom attached to each carbon atom and with all of the atoms probably lying in a plane. Two possibilities exist: the chlorine atoms may lie on the same side of the line joining the carbon atoms (*cis*-form) or they may lie on opposite sides (*trans*-form). The chlorine-chlorine separations are quite different in the two cases. The latest electron-diffraction results show that one compound has a Cl−Cl separation of 3.22A while the other has the value 4.27A; accordingly the former is the *cis*-compound.

The characteristic values of the angles between the bonds which one atom forms with other atoms have been extensively studied. Wierl[111] confirmed the tetrahedral angle (109° 28′) between the carbon atom single bonds by studying a series of hydrocarbons. Possible deviations from this value in the case of an unsymmetrically substituted atom have been investigated; examples are methylene chloride (CH_2Cl_2) and chloroform ($CHCl_3$)[110] in which the Cl−C−Cl angles are increased only about 3° above the angle in the symmetrical compound CCl_4. The trivalent molecules of the fifth group elements (N, P, As) are pyramidal with bond angles from about 100° to 110° (see $N(CH_3)_3$, PF_3, PCl_3, AsF_3, $AsCl_3$ in Table IV) except for the interesting cases of P_4 and As_4[103] with 60° angles. The oxygen bond angle has been studied in OF_2, Cl_2O, $(CH_3)_2O$, 1,4-dioxane, paraldehyde, CH_3ONH_2, and 4,4′-diiododiphenyl ether and varies from about 100° to 118° according to the size of the attached atoms or groups.

The length of the bonds which an atom forms with other atoms is even more important than the angles. The bond distance is characteristic not only of the chemical elements involved but also of the type of bond formed. Tables of atomic radii for a given bond type[57] have been formed such that the sum of the radii for two elements represents the interatomic distance when a bond of the given type has been formed between atoms of the respective elements. The observed bond distance then serves as a criterion for the bond type (which may be single, double, or triple covalent, resonating covalent, ionic, mixed ionic and covalent, etc.).

A particular case in which electron diffraction data have been used in determining bond types

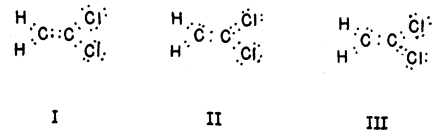

I II III

FIG. 11. Electron-pair bond arrangements in 1,1-dichloroethylene.

is that of the chloroethylenes.[71] The conventional bond arrangement in a molecule of any of the chloroethylenes places a double electron-pair bond between the two carbon atoms and single electron-pair bonds between the carbon atoms and the hydrogen and chlorine atoms. Other arrangements are compatible with the rules governing the formulation of bonding in molecules. In these the double bond occupies the C−Cl position. These possibilities are illustrated for 1,1-dichloroethylene in Fig. 11.

If structure I alone correctly represented the normal state of the molecule the carbon-carbon distance would be about 1.38A as observed for ethylene type compounds in general and the carbon-chlorine bond distance would be about 1.76A as observed in the chlorinated methanes. Structures II and III without I could not represent the normal state (because I has a little lower potential energy) but if they make an appreciable contribution to the normal state the observed bond distances will be different from those predicted for Structure I. Since II and III are physically indistinguishable the two carbon-chlorine bond distances will have the same value, which would be 1.64A if I, II, and III were equally important. The observed distances in 1,1-dichloroethylene are C−C=1.38A and C−Cl=1.69±0.02A. This result shows that Structure I is not an adequate representation of the molecule; moreover, the empirical relation[68] between bond distance and double bond character indicates that each carbon-chlorine bond is 14 percent double and 86 percent single in character. This can be interpreted in terms of a resonance of the double bond among the three possible positions in which the relative time spent in each position can be determined from the percentages quoted. The details of this application together with its extension to other resonating molecules by means of electron diffraction data is given by Pauling, Brockway, and Beach.[58]

Many other structural problems have been treated by various authors with the aid of electron diffraction results combined in some cases with the results of other experimental methods. For these the reader is referred to the literature cited in Table IV.

In Table IV are listed all of the substances for which electron diffraction investigations of the vapor have been reported. The table has been divided into three classifications: inorganic molecules (not containing carbon), aliphatic molecules (which includes all of the carbon compounds reported except benzene derivatives), and aromatic molecules (benzene derivatives).

The inorganic molecules have been sub-divided according to the group in the chemical periodic table to which the central atom of the molecule belongs. The columns of the table show the chemical formula, a symbol designating the structure type, a word characterizing the configuration of the molecule, the observed bond distances and angles and the literature references to all of the investigations which have been carried out on each substance. Since it is not possible to give a complete report of each investigation the structural data in the table represent the most probable values, which have been chosen after consideration of all of the reports on a given compound. The structure type symbol of the second column shows the number of atoms in the molecule together with Schoenflies point group symbol[69] representing the symmetry of the molecule. For a given number of atoms the symmetry operators of the point group afford a unique description of the molecular configuration in all of the compounds listed with only one or two exceptions; for these cases the necessary extra information is given. The description of the configuration given in the third column is intended as an aid in interpreting the structure type symbol; "tetrahedral" and "octahedral" as used here indicate *regular* tetrahedral or octahedral configurations. The bond distances are the separations of the central from the outer atoms; other interatomic distances can be calculated from these and the configurations. Bond angles on the central atom are also given whenever an extra parameter is required. The

molecule $B_3N_3H_6$ has no central atom but the regular hexagonal ring of atoms is fixed by giving the B—N separation. The molecules P_4 and As_4 also have no central atoms and the distances reported refer to the bonds formed along the edges of the tetrahedron.

The distances given in the table represent the most probable values as determined by electron diffraction methods and the uncertainty is an estimated probable error. The errors enclosed in parentheses have been supplied by the writer either because the original report contained no estimate of the error or because in the judgment of the writer the estimate was too small. When the distance value as well is enclosed in parentheses it is felt that the true value lies entirely outside of the range allowed in the original report. This judgment is always based on the results of investigations on similar compounds and it is highly probable that a more careful reinvestigation of the same compound would lead to a corrected value. In the cases where more careful reinvestigations have been made only the later result is given in the table. When the distance (or angle) value is given without any estimate of the error the value was assumed (generally from the results of experiments on related compounds) in order to reduce the number of parameters to be treated. In a few cases compounds are listed without structural data because the conclusions reached by the original investigators are not warranted by the experimental evidence.

In the table of aliphatic molecules the subdivision is made according to the number of carbon atoms, and within the C_2 group according to ethane, ethylene, and acetylene derivatives. No structure type symbol is given but the configuration is often described in a word. The C—H bond distance has been variously assumed to have values from 1.04A to 1.10A. This distance and the positions of the hydrogen atoms cannot be accurately determined because of the more powerfully scattering atoms in the molecule or else because the whole molecule is too light to give sharp interference patterns; accordingly the C—H distance is not given for any of the compounds. The ethylene derivatives are understood to be planar. The manner of reporting the parameters is the same as for the inorganic molecules.

The table of aromatic molecules includes all of the benzene derivatives for which the results of structural investigations have been published, the benzene ring is planar and its size in various derivatives has generally been assumed as indicated. It may be noted that in the molecules with heavy substituent atoms the C—X distance reported is directly dependent on the size assumed for the benzene ring.

In the literature references are listed all of the papers reporting on results of diffraction experiments with high velocity electrons and gas molecules.

References

1. P. Lenard, Ber. Berl. Akad. 1893.
2. C. J. Davisson and C. H. Kunsman, Phys. Rev. **22**, 242 (1923).
3. C. J. Davisson and L. H. Germer, Phys. Rev. **30**, 705 (1927).
4. L. de Broglie, Thesis, Paris (1924); Phil. Mag. **47**, 446 (1924).
5. G. P. Thomson, Proc. Roy. Soc. (London) **A117**, 600; **A119**, 651 (1928).
6. S. Kikuchi, Jap. J. Physics **5**, 83 (1928).
7. (a) N. F. Mott, Proc. Camb. Soc. **25**, 304 (1929); (b) Proc. Roy. Soc. (London) **A127**, 658 (1930).
8. G. P. Thomson, Proc. Roy. Soc. (London) **A125**, 352 (1929).
9. H. Mark and R. Wierl, Zeits. f. Physik **60**, 741 (1930).
10. R. Wierl, Ann. d. Physik **8**, 521 (1931).
11. The earlier work on diffraction of *slow* electrons by gas molecules is reviewed in J. Hengstenberg and K. Wolf, Hand u. Jahrbuch d. chem. Physik, Vol. 6, part 1A, pp. 129–138 (Akad. Verlagsges., Leipzig, 1935). References to later work are the following: F. L. Arnot, Proc. Roy. Soc. (London) **A144**, 360 (1934); F. L. Arnot and J. C. McLauchlan, Proc. Roy. Soc. (London) **A146**, 662 (1934); E. C. Childs and A. H. Woodcock, Proc. Roy. Soc. (London) **A146**, 199 (1934); H. S. W. Massey and E. C. Bullard, Proc. Cambridge Phil. Soc. **29**, 511 (1933); C. B. O. Mohr and F. H. Nicoll, Proc. Roy. Soc. (London) **A144**, 596 (1934); **A142**, 320, 647 (1933); S. N. Van Voorhis, Phys. Rev. **46**, 480 (1934); G. M. Webb, Phys. Rev. **47**, 384 (1935).
12. H. S. W. Massey, Proc. Roy. Soc. (London) **A129**, 616 (1930); H. S. W. Massey and C. B. O. Mohr, Proc. Roy. Soc. (London), **A135**, 258 (1932).
13. An extensive symposium on diffraction by solids is reported in Trans. Faraday Soc. **31**, 1043 (1935).

14. L. Pauling and L. O. Brockway, J. Chem. Phys. **2**, 867 (1934).
15. N. F. Mott and H. S. W. Massey, Theory of Atomic Collisions (Oxford Press, 1933), cf. Chapter VI.
16. H. Bethe, Ann. d. Physik **5**, 325 (1930).
17. For a discussion of the non-converging integral introduced by substitution of the first term of (11) in (9) or (10), see reference 7(b), page 662.
18. (a) R. W. James and G. W. Brindley, Zeits. f. Krist. **78**, 370 (1931); (b) L. Pauling and J. Sherman, Zeits. f. Krist. **81**, 28 (1932).
19. J. Macdougall, Proc. Roy. Soc. (London) **A136**, 549 (1932).
20. P. Debye, Ann. d. Physik **46**, 809 (1915).
21. P. Ehrenfest, Amsterdam Acad. **23**, 1132 (1915).
22. H. S. W. Massey and C. B. O. Mohr, Proc. Roy. Soc. (London) **A135**, 258 (1932).
23. P. M. Morse, Physik. Zeits. **33**, 443 (1932).
24. W. Heisenberg, Physik. Zeits. **32**, 737 (1931).
25. L. Bewilogua, Physik. Zeits. **32**, 740 (1931).
26. R. W. James, Physik. Zeits. **33**, 737 (1932).
27. W. van der Grinten, Physik. Zeits. **34**, 609 (1933).
28. C. Degard, J. Pierard, and W. van der Grinten, Nature **136**, 142 (1935).
29. M. C. Neuberger, Zeits. f. Krist. **93**, 1 (1936).
30. D. H. Sloan, R. L. Thornton, and F. A. Jenkins, R. S. I. **6**, 80 (1935).
31. K. C. D. Hickman, J. Frank. Inst. **221**, 215 (1936).
32. H. de Laszlo, Proc. Roy. Soc. (London) **A146**, 662 (1934).
33. V. E. Cosslett, Trans. Faraday Soc. **30**, 981 (1934).
34. H. Seemann, Ergeb. techn. Roentgenkunde **3**, 95 (1933); Zeits. f. Physik **92**, 270 (1934).
35. W. Grether, Ann. d. Physik **26**, 1 (1936).
36. (a) High velocity electrons—A. Becker and E. Kipphan, Ann. d. Physik **10**, 15 (1931); (b) Intermediate velocities—M. Nacken, Physik. Zeits. **31**, 296 (1930); W. Seitz and G. Harig, Physik. Zeits. **30**, 758 (1929); (c) Low velocity—V. Weidner, Ann. d. Physik **12**, 239 (1932).
37. L. Pauling and L. O. Brockway, J. Chem. Phys. **2**, 867 (1934).
38. L. O. Brockway and F. T. Wall, J. Am. Chem. Soc. **56**, 2373 (1934).
39. C. E. St. John and L. W. Ware, Astrophys. J. **44**, 35 (1916).
40. L. O. Brockway and L. Pauling, Proc. Nat. Acad. Sci. **19**, 68 (1933).
41. V. E. Cosslett, Trans. Faraday Soc. **30**, 981 (1934).
42. J. Sherman, Zeits. f. Krist. **85**, 404 (1933).
43. These tables have never been published but are available from Dr. Paul Cross, Stanford University. They give $(\sin ax)/ax$ for $0.80 \leq a \leq 4.00$ at intervals of 0.01, for values of x up to 40, and $4.02 \leq a \leq 8.00$ at intervals of 0.02, for values of x up to 20, the intervals for x being 0.2.
44. L. R. Maxwell, S. B. Hendricks, and V. M. Mosley, J. Chem. Phys. **3**, 699 (1935).
45. C. Degard and W. van der Grinten, Bull. Soc. Roy. Sci. (Liège), No. 4–5, 1 (1935).
46. S. B. Hendricks, L. R. Maxwell, V. L. Mosley, and M. E. Jefferson, J. Chem. Phys. **1**, 549 (1933).
47. Trendelenburg, Naturwiss. **21**, 173 (1933); Trendelenburg and Franz, Veroff. Siemens Konzern **13**, 48 (1934).
48. F. W. Sears, J. Opt. Soc. Am. **25**, 162 (1935).
49. L. Pauling and L. O. Brockway, J. Am. Chem. Soc. **57**, 2684 (1935).
50. L. O. Brockway, Proc. Nat. Acad. Sci. **19**, 303, 868 (1933).
51. P. Cross and L. O. Brockway, J. Chem. Phys. **3**, 821 (1935).
52. L. Bewilogua, Physik. Zeits. **33**, 688 (1932).
53. P. Debye, L. Bewilogua, and F. Ehrhardt, Physik. Zeits. **30**, 84 (1929).
54. P. Debye, Physik. Zeits. **30**, 524 (1929).
55. P. Debye, Physik. Zeits. **31**, 419 (1930); L. Bewilogua, Physik. Zeits. **32**, 265 (1931).
56. R. Wierl, *Leipziger Vorträge* (1930), p. 13.
57. For example, see L. Pauling and M. L. Huggins, Zeits. f. Krist. **87**, 205 (1934).
58. L. Pauling, L. O. Brockway, and J. Y. Beach, J. Am. Chem. Soc. **57**, 2705 (1935).
59. Stereographic projections of the crystallographic point groups showing the symmetry operators are given by P. Ewald, Handbuch d. Physik, 2nd ed., Vol. XXIII, part 2 (Julius Springer, Berlin, 1933), pp. 226–233.
60. H. Boersch, Sitzberich. Acad. Wiss. Wien **144**, 1 (1935).
61. H. Boersch, Monatsh. **65**, 311 (1935).
62. H. Boersch, Naturwiss. **22**, 172 (1934).
63. H. Braune and S. Knoke, Zeits. f. physik. Chemie **B23**, 163 (1933).
64. H. Braune and S. Knoke, Naturwiss. **21**, 349 (1933).
65. H. Braune and S. Knoke, Zeits. f. physik. Chemie **B21**, 297 (1933).
66. L. O. Brockway, J. Am. Chem. Soc. **57**, 958 (1935).
67. L. O. Brockway, Proc. Nat. Acad. Sci. **19**, 868 (1933).
68. L. O. Brockway, Proc. Nat. Acad. Sci. **19**, 303 (1933).
69. L. O. Brockway, in publication.
70. L. O. Brockway and J. Y. Beach, in publication.
71. L. O. Brockway, J. Y. Beach, and L. Pauling, J. Am. Chem. Soc. **57**, 2693 (1935).
72. L. O. Brockway and P. C. Cross, J. Chem. Phys. **3**, 828 (1935).
73. L. O. Brockway and H. O. Jenkins, in publication.
74. L. O. Brockway and H. Levy, in publication.
75. L. O. Brockway and K. Palmer, in publication.
76. L. O. Brockway and L. Pauling, Proc. Nat. Acad. Sci. **19**, 860 (1933).
77. L. O. Brockway and L. Pauling, Proc. Nat. Acad. Sci. **19**, 68 (1933).
78. L. O. Brockway and F. T. Wall, J. Am. Chem. Soc. **56**, 2373 (1934).
79. Luis Bru, Rev. Acad. Cienc. Madrid **30**, 586 (1933).
80. Luis Bru, Anales soc. espan. fis. quim. **31**, 115 (1933).
81. Luis Bru, Anales soc. espan. fis. quim. **30**, 483, 486 (1932).

82. D. C. Carpenter and L. O. Brockway, J. Am. Chem. Soc., in publication.
83. V. E. Cosslett, Trans. Faraday Soc. **30**, 981 (1934).
84. V. E. Cosslett, and H. G. de Laszlo, Nature **134**, 63 (1934).
85. P. Cross and L. O. Brockway, J. Chem. Phys. **3**, 821 (1935).
86. C. Degard, Compt. Rend. **201**, 951 (1935).
87. C. Degard, J. Pierard and W. van der Grinten, Nature **136**, 142 (1935).
88. C. Degard and W. van der Grinten, Bull. Soc. Roy. Sci. Liège, Nos. 4-5, 1 (1935).
89. R. W. Dornte, J. Am. Chem. Soc. **55**, 4126 (1933).
90. R. W. Dornte, J. Chem. Phys. **1**, 630 (1933).
91. R. W. Dornte, J. Chem. Phys. **1**, 566 (1933).
92. W. Grether, Ann. d. Physik **26**, 1 (1936).
93. S. B. Hendricks, L. R. Maxwell, V. L. Mosley, and M. E. Jefferson, J. Chem. Phys. **1**, 549 (1933).
94. J. Hengstenberg and L. Bru, Anales soc. espan. fis. quim. **30**, 341 (1932).
95. P. L. F. Jones, Trans. Faraday Soc. **31**, 1036 (1935).
96. H. de Laszlo, Nature **135**, 474 (1935).
97. H. de Laszlo, Proc. Roy. Soc. (London), **A146**, 672, 690 (1934).
98. H. de Laszlo, Nature, **131**, 803 (1933).
99. H. Mark and R. Wierl, Zeits. f. Elektrochem. **36**, 675 (1930).
100. H. Mark and R. Wierl, Zeits. f. Physik **60**, 741 (1930).
101. H. Mark and R. Wierl, Naturwiss. **18**, 778 (1930).
102. H. Mark and R. Wierl, Naturwiss. **18**, 205 (1930).
103. L. R. Maxwell, S. B. Hendricks, and V. M. Mosley, J. Chem. Phys. **3**, 699 (1935).
104. L. R. Maxwell, V. M. Mosley, and Lola S. Deming, J. Chem. Phys. **2**, 331 (1934).
105. L. Pauling and L. O. Brockway, in publication.
106. L. Pauling and L. O. Brockway, J. Am. Chem. Soc. **57**, 2684 (1935).
107. L. Pauling and L. O. Brockway, Proc. Nat. Acad. Sci. **20**, 336 (1934).
108. L. Pauling and L. O. Brockway, J. Chem. Phys. **2**, 867 (1934).
109. A. Stock and R. Wierl, Zeits. f. anorg. u. allgem. Chemie **203**, 228 (1931).
110. L. E. Sutton and L. O. Brockway, J. Am. Chem. Soc. **57**, 473 (1935).
111. R. Wierl, Ann. d. Physik **13**, 453 (1932).
112. R. Wierl, Ann. d. Physik **8**, 521 (1931).
113. R. Wierl, Physik. Zeits. **31**, 1028 (1930).
114. R. Wierl, Verh. D. Phys. Ges. **11**, 29 (1930).
115. R. Wierl, *Leipziger Vorträge* (1930), p. 13.
116. R. Wierl, Physik. Zeits. **31**, 366 (1930).
117. P. G. Ackermann and J. E. Mayer, J. Chem. Phys. **4**, 377 (1936).
118. S. H. Bauer, J. Chem. Phys. **4**, July (1936).
119. S. S. Lu, Chinese J. Phys. **1**, 51 (1933).
120. W. van der Grinten and H. Brasseur, Nature **137**, 657 (1936).

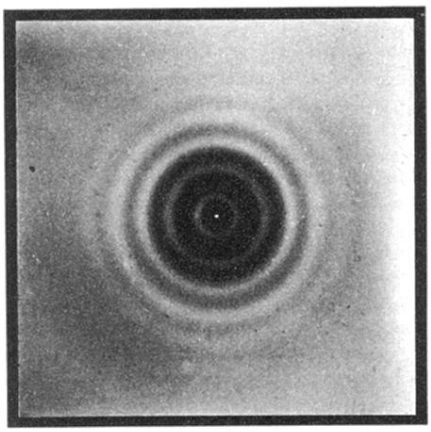

FIG. 6. Eleetron diffraction photograph of As_4 vapor. This photograph was taken by Dr. L. R. Maxwell of the U. S. Department of Agriculture.

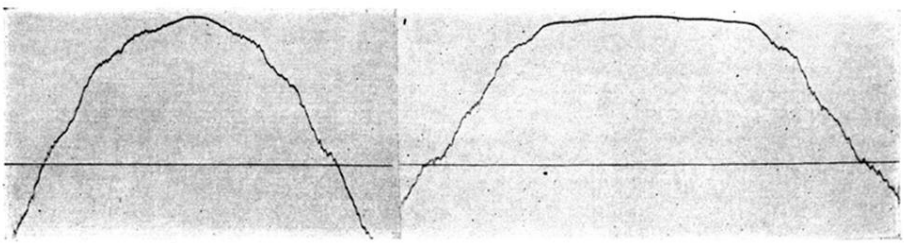

FIG. 8. Microphotometer records of CCl_4 photographs, (A) (left) showing the first three and (B) (right) showing the first five apparent maxima.